Linear Inverse Problems, Quadratic Spectral Estimators & Spatiospectral Concentration: Earth, Planets & Space

Frederik J Simons │ Alain Plattner

Princeton University │ The University of Alabama

Mark A. Wieczorek │ F. A. Dahlen │ J. C. Hawthorne │ Volker Michel
Shin-Chan Han │ Ciarán Beggan │ Kevin W. Lewis │ Chris Harig

Determining the Depth of Jupiter's Great Red Spot with Juno: A Slepian Approach

Eli Galanti[1], Yohai Kaspi[1], Frederik J. Simons[2,6], Daniele Durante[3], Marzia Parisi[4], and Scott J. Bolton[5]

[1] Department of Earth and Planetary Sciences, Weizmann Institute of Science, Rehovot, Israel; eli.galanti@weizmann.ac.il
[2] Department of Geosciences, Princeton University, NJ, USA
[3] Dipartimento di Ingegneria Meccanica e Aerospaziale, Sapienza Università di Roma, Rome, Italy
[4] Jet Propulsion Laboratory, California Institute of Technology, Pasadena, CA, USA
[5] Southwest Research Institute, San Antonio, TX, USA

Determining the Depth of Jupiter's Great Red Spot with Juno: A Slepian Approach

Eli Galanti[1] ⓘ, Yohai Kaspi[1] ⓘ, Frederik J. Simons[2,6] ⓘ, Daniele Durante[3] ⓘ, Marzia Parisi[4] ⓘ, and Scott J. Bolton[5] ⓘ

[1] Department of Earth and Planetary Sciences, Weizmann Institute of Science, Rehovot, Israel; eli.galanti@weizmann.ac.il

[2] Department of Geosciences, Princeton University, NJ, USA

[3] Dipartimento di Ingegneria Meccanica e Aerospaziale, Sapienza Università di Roma, Rome, Italy

[4] Jet Propulsion Laboratory, California Institute of Technology, Pasadena, CA, USA

[5] Southwest Research Institute, San Antonio, TX, USA

The Mercury gravity field, orientation, love number, and ephemeris from the MESSENGER radiometric tracking data[☆]

A.S. Konopliv[*], R.S. Park, A.I. Ermakov

Jet Propulsion Laboratory, California Institute of Technology, Pasadena, CA 91109, USA

Determining the Depth of Jupiter's Great Red Spot with Juno: A Slepian Approach

Eli Galanti[1], Yohai Kaspi[1], Frederik J. Simons[2,6], Daniele Durante[3], Marzia Parisi[4], and Scott J. Bolton[5]

[1] Department of Earth and Planetary Sciences, Weizmann Institute of Science, Rehovot, Israel; eli.galanti@weizmann.ac.il
[2] Department of Geosciences, Princeton University, NJ, USA
[3] Dipartimento di Ingegneria Meccanica e Aerospaziale, Sapienza Università di Roma, Rome, Italy
[4] Jet Propulsion Laboratory, California Institute of Technology, Pasadena, CA, USA
[5] Southwest Research Institute, San Antonio, TX, USA

The Mercury gravity field, orientation, love number, and ephemeris from the MESSENGER radiometric tracking data[☆]

A.S. Konopliv[*], R.S. Park, A.I. Ermakov

Jet Propulsion Laboratory, California Institute of Technology, Pasadena, CA 91109, USA

Evidence of non-uniform crust of Ceres from Dawn's high-resolution gravity data

R. S. Park[1✉], A. S. Konopliv[1], A. I. Ermakov[1,2], J. C. Castillo-Rogez[1], R. R. Fu[3], K. H. G. Hughson[4], T. H. Prettyman[5], C. A. Raymond[1], J. E. C. Scully[1], H. G. Sizemore[5], M. M. Sori[6], A. T. Vaughan[1], G. Mitri[7,8], B. E. Schmidt[4] and C. T. Russell[9]

Determining the Depth of Jupiter's Great Red Spot with Juno: A Slepian Approach

Eli Galanti[1] , Yohai Kaspi[1] , Frederik J. Simons[2,6] , Daniele Durante[3] , Marzia Parisi[4] , and Scott J. Bolton[5]
[1] Department of Earth and Planetary Sciences, Weizmann Institute of Science, Rehovot, Israel; eli.galanti@weizmann.ac.il
[2] Department of Geosciences, Princeton University, NJ, USA
[3] Dipartimento di Ingegneria Meccanica e Aerospaziale, Sapienza Università di Roma, Rome, Italy
[4] Jet Propulsion Laboratory, California Institute of Technology, Pasadena, CA, USA
[5] Southwest Research Institute, San Antonio, TX, USA

The Mercury gravity field, orientation, love number, and ephemeris from the MESSENGER radiometric tracking data[☆]

A.S. Konopliv[*], R.S. Park, A.I. Ermakov

Jet Propulsion Laboratory, California Institute of Technology, Pasadena, CA 91109, USA

Evidence of non-uniform crust of Ceres from Dawn's high-resolution gravity data

R. S. Park [1⊠], A. S. Konopliv[1], A. I. Ermakov[1,2], J. C. Castillo-Rogez[1], R. R. Fu[3], K. H. G. Hughson [4], T. H. Prettyman [5], C. A. Raymond [1], J. E. C. Scully[1], H. G. Sizemore [5], M. M. Sori [6], A. T. Vaughan[1], G. Mitri [7,8], B. E. Schmidt [4] and C. T. Russell[9]

Recipe for Inferring Subsurface Solar Magnetism via Local Mode Coupling Using Slepian Basis Functions

Srijan Bharati Das
Department of Geosciences, Princeton University, Princeton, NJ, USA; sbdas@princeton.edu

Functions cannot be bandlimited and spacelimited at the same time.

Localization in a nutshell

Functions cannot be bandlimited and spacelimited at the same time.

However, we can find a set of **bandlimited** functions that will optimize their *spatial concentration* to some spatial domain, and we can find a set of **spacelimited** functions that will minimize *spectral leakage* outside the bandlimit of interest.

Functions cannot be bandlimited and spacelimited at the same time.

However, we can find a set of **bandlimited** functions that will optimize their *spatial concentration* to some spatial domain, and we can find a set of **spacelimited** functions that will minimize *spectral leakage* outside the bandlimit of interest.

Functions cannot be bandlimited and spacelimited at the same time.

However, we can find a set of **bandlimited** functions that will optimize their *spatial concentration* to some spatial domain, and we can find a set of **spacelimited** functions that will minimize *spectral leakage* outside the bandlimit of interest.

We can use these "Slepian" functions as **windows**, for spectral analysis, or we can use them as a **(sparse) basis** to represent *geo*physical observables—on a sphere.

A brief history of Slepian functions — 1

In the 60s Slepian *et al.* solved the problem of concentrating a **bandlimited** signal

$$g(t) = \frac{1}{2\pi} \int_{-W}^{+W} G(\omega)\, e^{i\omega t}\, d\omega, \qquad |W| < \infty, \tag{1}$$

into a **time interval** $|t| \leq T$. The "Slepian functions" optimize the **concentration**

$$\lambda = \frac{\displaystyle\int_{-T}^{+T} g^2(t)\, dt}{\displaystyle\int_{-\infty}^{+\infty} g^2(t)\, dt}, \qquad 0 < \lambda < 1. \tag{2}$$

In the 60s Slepian *et al.* solved the problem of concentrating a **bandlimited** signal

$$g(t) = \frac{1}{2\pi} \int_{-W}^{+W} G(\omega)\, e^{i\omega t}\, d\omega, \qquad |W| < \infty, \tag{1}$$

into a **time interval** $|t| \leq T$. The "Slepian functions" optimize the **concentration**

$$\lambda = \frac{\displaystyle\int_{-T}^{+T} g^2(t)\, dt}{\displaystyle\int_{-\infty}^{+\infty} g^2(t)\, dt}, \qquad 0 < \lambda < 1. \tag{2}$$

They are **eigenfunctions** of a Fredholm integral equation,

$$\int_{-T}^{T} \left[\frac{\sin W(t - t')}{\pi(t - t')} \right] g(t')\, dt' = \lambda\, g(t). \tag{3}$$

Similarly, *two*-dimensional Slepian functions are bandlimited Fourier expansions

$$g(\mathbf{x}) = \frac{1}{(2\pi)^2} \int_{\mathcal{K}} G(\mathbf{k})\, e^{i\mathbf{k}\cdot\mathbf{x}}\, d\mathbf{k}, \qquad |\mathcal{K}| < \infty, \tag{4}$$

that concentrate into a finite **spatial** region $\mathcal{R} \in \mathbb{R}^2$ of area A by maximizing

$$\lambda = \frac{\displaystyle\int_{\mathcal{R}} g^2(\mathbf{x})\, d\mathbf{x}}{\displaystyle\int_{-\infty}^{+\infty} g^2(\mathbf{x})\, d\mathbf{x}}, \qquad 0 < \lambda < 1. \tag{5}$$

A brief history of Slepian functions — 2

Similarly, *two*-dimensional Slepian functions are bandlimited Fourier expansions

$$g(\mathbf{x}) = \frac{1}{(2\pi)^2} \int_{\mathcal{K}} G(\mathbf{k}) \, e^{i\mathbf{k}\cdot\mathbf{x}} \, d\mathbf{k}, \qquad |\mathcal{K}| < \infty, \tag{4}$$

that concentrate into a finite **spatial** region $\mathcal{R} \in \mathbb{R}^2$ of area A by maximizing

$$\lambda = \frac{\displaystyle\int_{\mathcal{R}} g^2(\mathbf{x}) \, d\mathbf{x}}{\displaystyle\int_{-\infty}^{+\infty} g^2(\mathbf{x}) \, d\mathbf{x}}, \qquad 0 < \lambda < 1. \tag{5}$$

These are also **eigenfunctions** of a Fredholm integral equation,

$$\int_{\mathcal{R}} \left[\frac{1}{(2\pi)^2} \int_{\mathcal{K}} e^{i\mathbf{k}\cdot(\mathbf{x}-\mathbf{x}')} \, d\mathbf{k} \right] g(\mathbf{x}') \, d\mathbf{x}' = \lambda g(\mathbf{x}). \tag{6}$$

On a **sphere**, Slepian functions are bandlimited *spherical-harmonic* expansions

$$g(\hat{\mathbf{r}}) = \sum_{l=0}^{L} \sum_{m=-l}^{l} g_{lm} Y_{lm}(\hat{\mathbf{r}}), \qquad L < \infty, \tag{7}$$

that are concentrated within a region $R \in \Omega$ by optimizing the energy ratio

$$\lambda = \frac{\displaystyle\int_R g^2(\hat{\mathbf{r}})\, d\Omega}{\displaystyle\int_\Omega g^2(\hat{\mathbf{r}})\, d\Omega}, \qquad 0 < \lambda < 1. \tag{8}$$

A brief history of Slepian functions — 3

On a **sphere**, Slepian functions are bandlimited *spherical-harmonic* expansions

$$g(\hat{\mathbf{r}}) = \sum_{l=0}^{L} \sum_{m=-l}^{l} g_{lm} Y_{lm}(\hat{\mathbf{r}}), \qquad L < \infty, \tag{7}$$

that are concentrated within a region $R \in \Omega$ by optimizing the energy ratio

$$\lambda = \frac{\displaystyle\int_{R} g^2(\hat{\mathbf{r}})\, d\Omega}{\displaystyle\int_{\Omega} g^2(\hat{\mathbf{r}})\, d\Omega}, \qquad 0 < \lambda < 1. \tag{8}$$

They are **eigenfunctions** of a Fredholm equation, with P_l a Legendre function,

$$\int_{R} \left[\sum_{l=0}^{L} \left(\frac{2l+1}{4\pi} \right) P_l(\hat{\mathbf{r}} \cdot \hat{\mathbf{r}}') \right] g(\hat{\mathbf{r}}')\, d\Omega' = \lambda\, g(\hat{\mathbf{r}}). \tag{9}$$
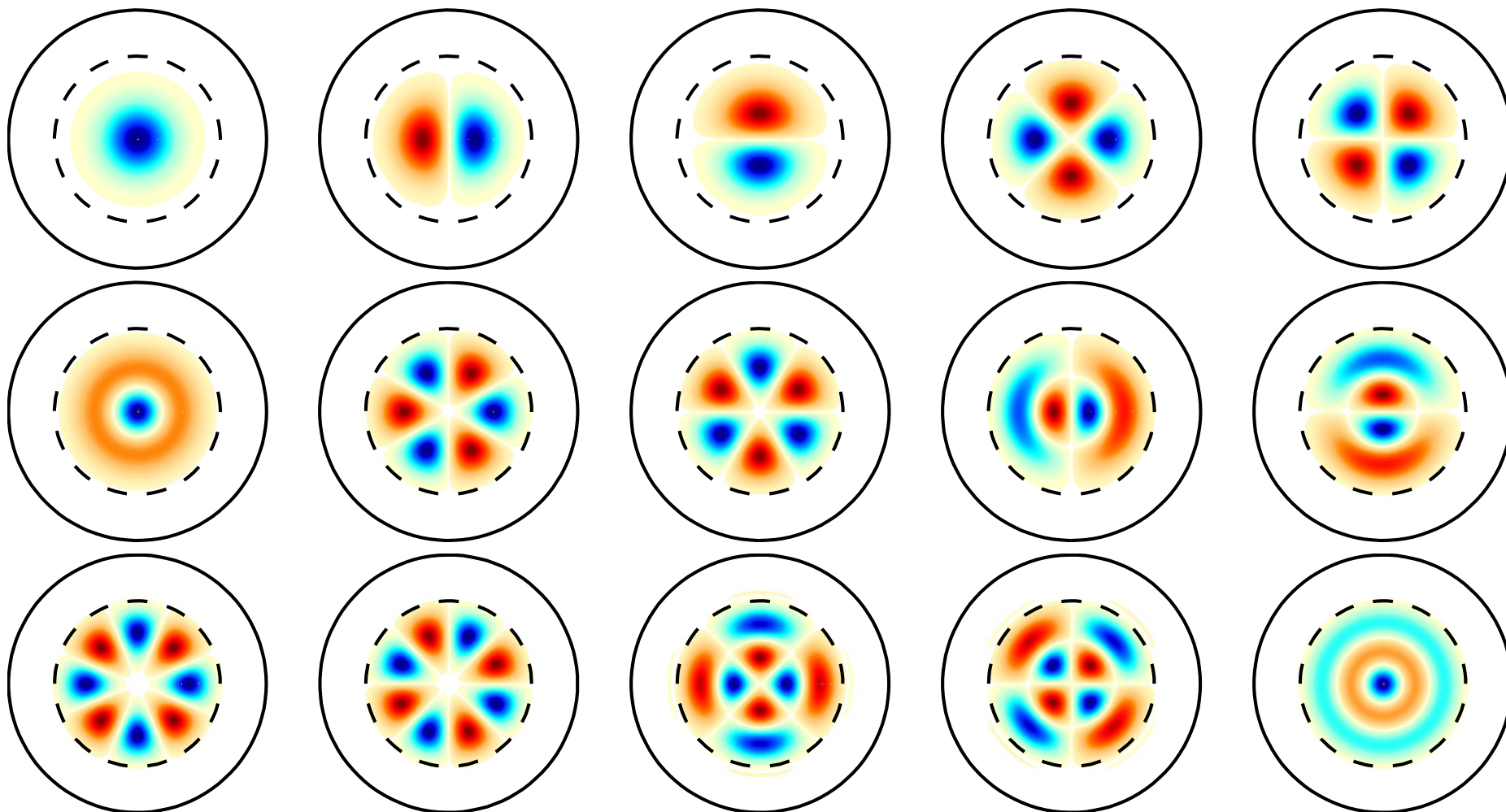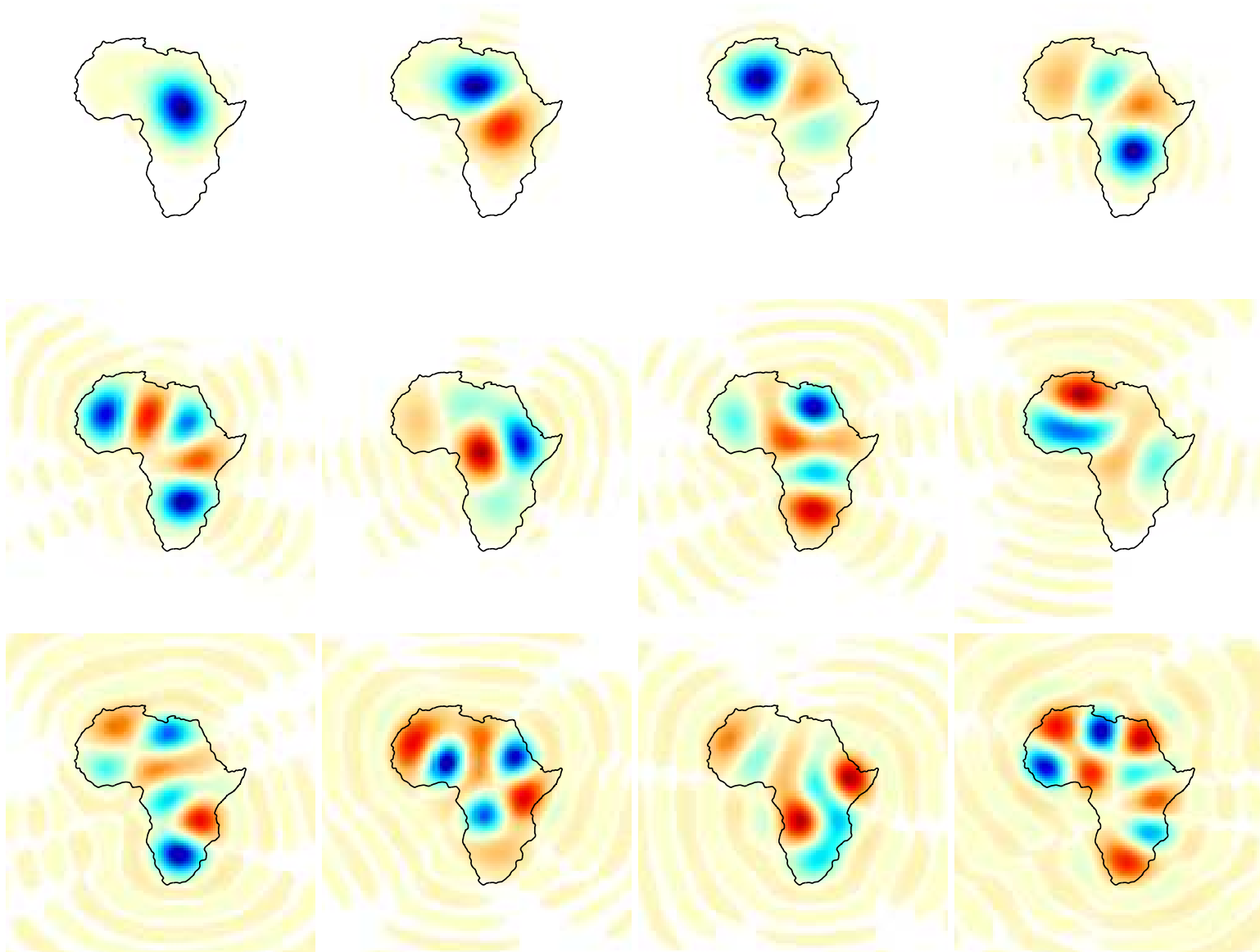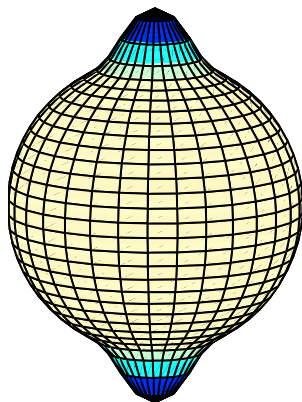
$\lambda_1 = 1.000 \times 10^{-00}$

$\lambda_2 = 1.000 \times 10^{-00}$
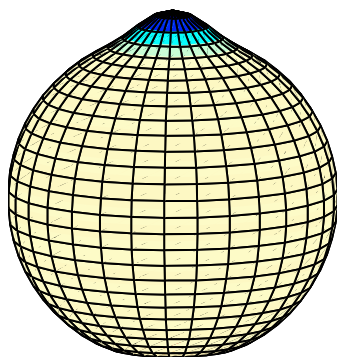
$\lambda_3 = 9.997 \times 10^{-01}$
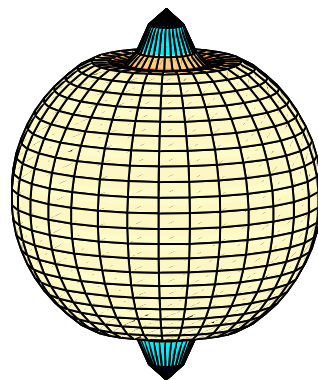
$\lambda_4 = 9.994 \times 10^{-01}$
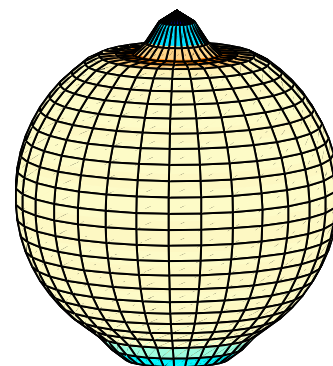
$\lambda_{16} = 4.857 \times 10^{-13}$
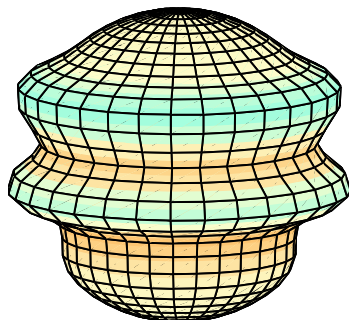
$\lambda_{17} = 3.124 \times 10^{-16}$
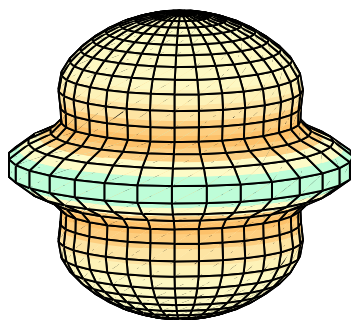
$\lambda_{18} = 1.748 \times 10^{-17}$
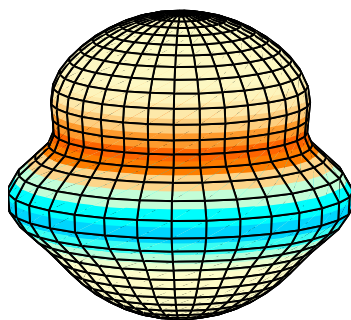
$\lambda_{19} = 2.750 \times 10^{-21}$
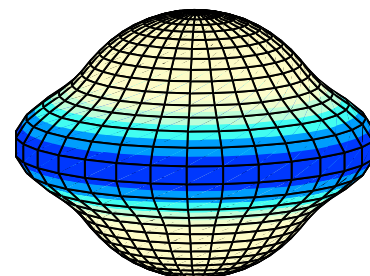
The integral-equation kernels are all *spectrally bandlimited spatial delta functions* that are "reproducing kernels" for the bandlimited functions of the kinds considered:

$$D(t, t') \;=\; \frac{1}{2\pi} \int_{-W}^{+W} e^{i\omega (t-t')} \, d\omega, \quad \mathrm{tr}\{D\} = 2\frac{TW}{\pi}, \tag{10}$$

The integral-equation kernels are all *spectrally bandlimited spatial delta functions* that are "reproducing kernels" for the bandlimited functions of the kinds considered:

$$D(t, t') = \frac{1}{2\pi} \int_{-W}^{+W} e^{i\omega(t-t')} \, d\omega, \quad \mathrm{tr}\{D\} = 2\frac{TW}{\pi}, \tag{10}$$

$$D(\mathbf{x}, \mathbf{x}') = \frac{1}{(2\pi)^2} \int_{\mathcal{K}} e^{i\mathbf{k}\cdot(\mathbf{x}-\mathbf{x}')} \, d\mathbf{k}, \quad \mathrm{tr}\{D\} = K^2 \frac{A}{4\pi}, \tag{11}$$

The integral-equation kernels are all *spectrally bandlimited spatial delta functions* that are "reproducing kernels" for the bandlimited functions of the kinds considered:

$$D(t, t') = \frac{1}{2\pi} \int_{-W}^{+W} e^{i\omega(t-t')} \, d\omega, \quad \mathrm{tr}\{D\} = 2\frac{TW}{\pi}, \tag{10}$$

$$D(\mathbf{x}, \mathbf{x}') = \frac{1}{(2\pi)^2} \int_{\mathcal{K}} e^{i\mathbf{k}\cdot(\mathbf{x}-\mathbf{x}')} \, d\mathbf{k}, \quad \mathrm{tr}\{D\} = K^2 \frac{A}{4\pi}, \tag{11}$$

$$D(\hat{\mathbf{r}}, \hat{\mathbf{r}}') = \sum_{l=0}^{L} \sum_{m=-l}^{m} Y_{lm}(\hat{\mathbf{r}}) Y_{lm}(\hat{\mathbf{r}}'), \quad \mathrm{tr}\{D\} = (L+1)^2 \frac{A}{4\pi}. \tag{12}$$

The integral-equation kernels are all *spectrally bandlimited spatial delta functions* that are "reproducing kernels" for the bandlimited functions of the kinds considered:

$$D(t, t') = \frac{1}{2\pi} \int_{-W}^{+W} e^{i\omega(t-t')} d\omega, \quad \mathrm{tr}\{D\} = 2\frac{TW}{\pi}, \quad (10)$$

$$D(\mathbf{x}, \mathbf{x}') = \frac{1}{(2\pi)^2} \int_{\mathcal{K}} e^{i\mathbf{k}\cdot(\mathbf{x}-\mathbf{x}')} d\mathbf{k}, \quad \mathrm{tr}\{D\} = K^2\frac{A}{4\pi}, \quad (11)$$

$$D(\hat{\mathbf{r}}, \hat{\mathbf{r}}') = \sum_{l=0}^{L} \sum_{m=-l}^{m} Y_{lm}(\hat{\mathbf{r}})Y_{lm}(\hat{\mathbf{r}}'), \quad \mathrm{tr}\{D\} = (L+1)^2\frac{A}{4\pi}. \quad (12)$$

Thus, the Slepian functions are **bases** for **bandlimited** geophysical processes **anywhere** (not just on the domain for which they were constructed, though, there, they will be a **sparse** basis). Their trace is a space-bandwidth joint "Shannon" *area*.

The integral-equation kernels are all *spectrally bandlimited spatial delta functions* that are "reproducing kernels" for the bandlimited functions of the kinds considered:

$$D(t,t') = \frac{1}{2\pi}\int_{-W}^{+W} e^{i\omega\,(t-t')}\,d\omega, \quad \text{tr}\{D\} = 2\frac{TW}{\pi}, \tag{10}$$

$$D(\mathbf{x},\mathbf{x}') = \frac{1}{(2\pi)^2}\int_{\mathcal{K}} e^{i\mathbf{k}\cdot(\mathbf{x}-\mathbf{x}')}\,d\mathbf{k}, \quad \text{tr}\{D\} = K^2\frac{A}{4\pi}, \tag{11}$$

$$D(\hat{\mathbf{r}},\hat{\mathbf{r}}') = \sum_{l=0}^{L}\sum_{m=-l}^{m} Y_{lm}(\hat{\mathbf{r}})Y_{lm}(\hat{\mathbf{r}}'), \quad \text{tr}\{D\} = (L+1)^2\frac{A}{4\pi}. \tag{12}$$

Thus, the Slepian functions are **bases** for **bandlimited** geophysical processes **anywhere** (not just on the domain for which they were constructed, though, there, they will be a **sparse** basis). Their trace is a space-bandwidth joint "Shannon" *area*.

Remember that the *trace* of an operator is the *sum* of all of its eigenvalues, N.

In the *spectral* domain, the Slepian functions are eigenfunctions of equations that have *spacelimited spectral delta functions* as kernels. On the **sphere**, we solve for the spherical harmonic expansion coefficients of the functions as

$$\sum_{l'=0}^{L}\sum_{m'=-l'}^{l'}\left[\int_R Y_{lm}Y_{l'm'}\,d\Omega\right]g_{l'm'}=\lambda g_{lm}, \qquad 0<\lambda<1. \tag{13}$$

A unified framework — 2

In the *spectral* domain, the Slepian functions are eigenfunctions of equations that have *spacelimited spectral delta functions* as kernels. On the **sphere**, we solve for the spherical harmonic expansion coefficients of the functions as

$$\sum_{l'=0}^{L} \sum_{m'=-l'}^{l'} \left[\int_R Y_{lm} Y_{l'm'} \, d\Omega \right] g_{l'm'} = \lambda g_{lm}, \qquad 0 < \lambda < 1. \tag{13}$$

We define the **spatiospectral localization kernel**, with eigenvalues λ, as

$$D_{lm,l'm'} = \int_R Y_{lm} Y_{l'm'} \, d\Omega, \qquad \mathrm{tr}\{\mathsf{D}\} = (L+1)^2 \frac{A}{4\pi}. \tag{14}$$
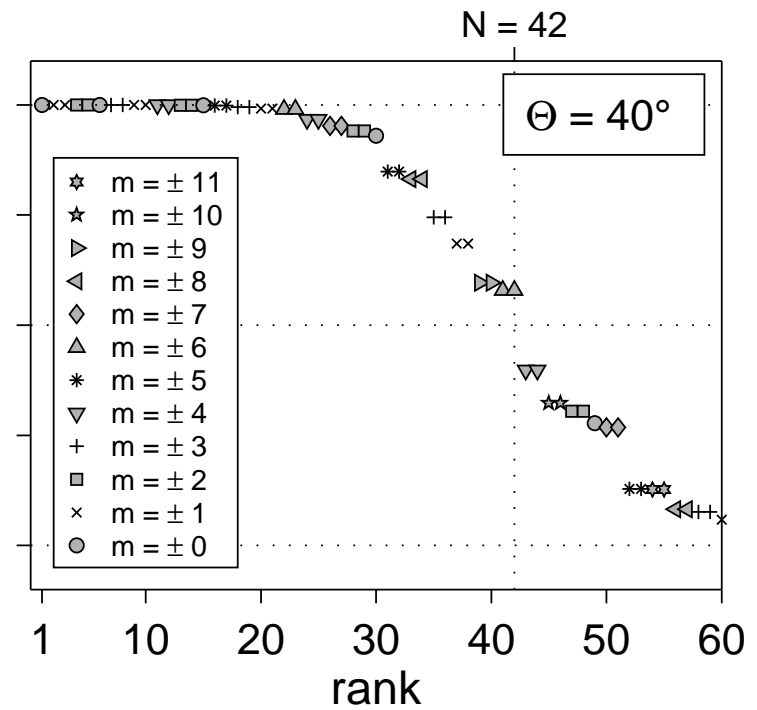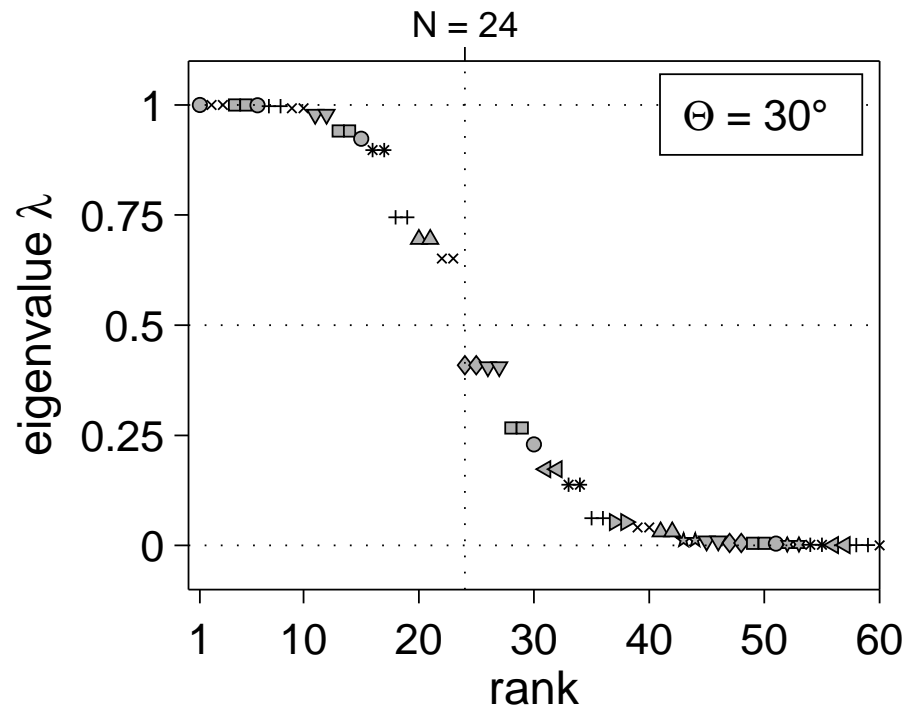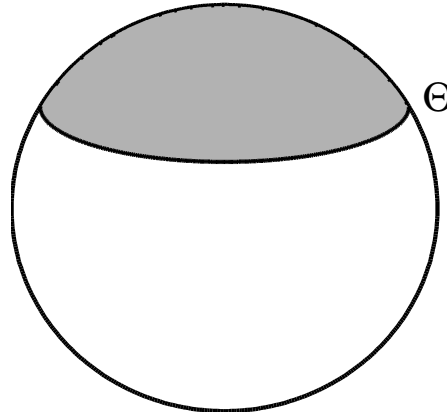
Many of the eigenvalues are very, very small. Thus, D may be hard to calculate— and even harder to *invert*.

And remember that the spatial region R can be *completely* arbitrary.
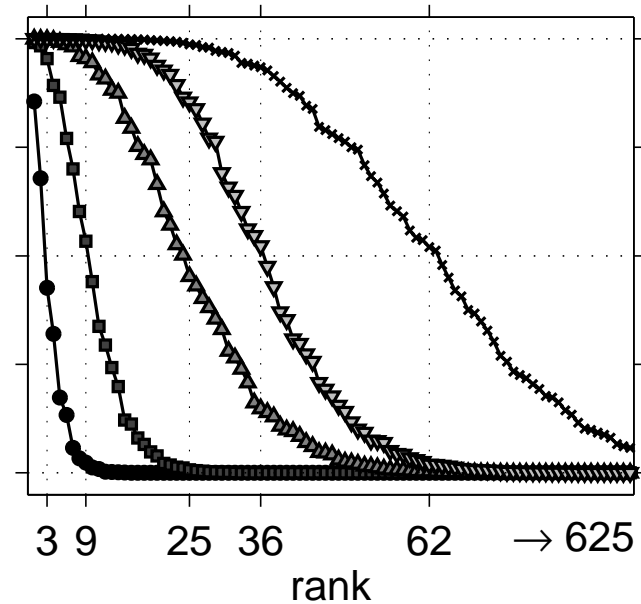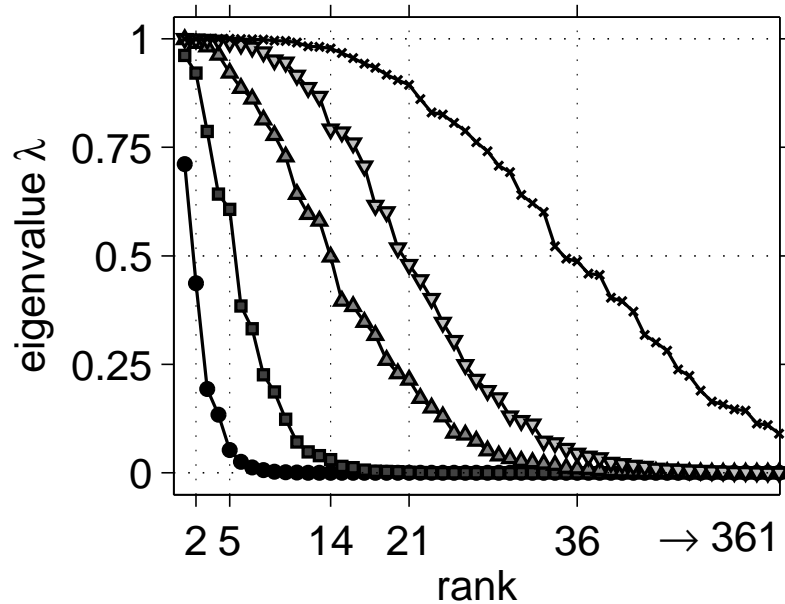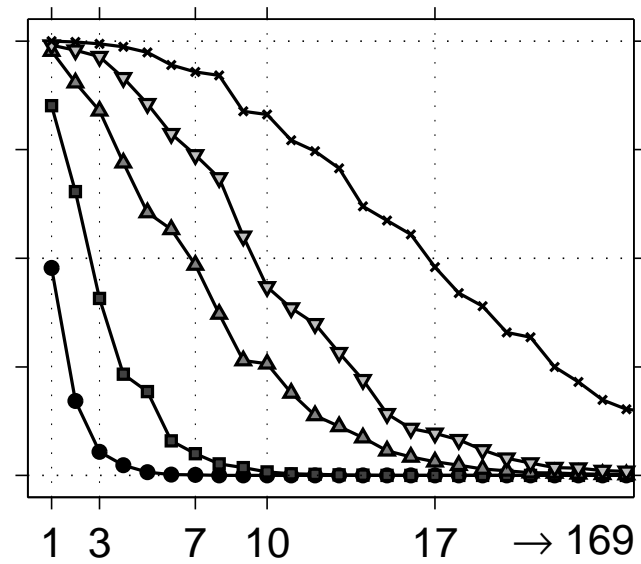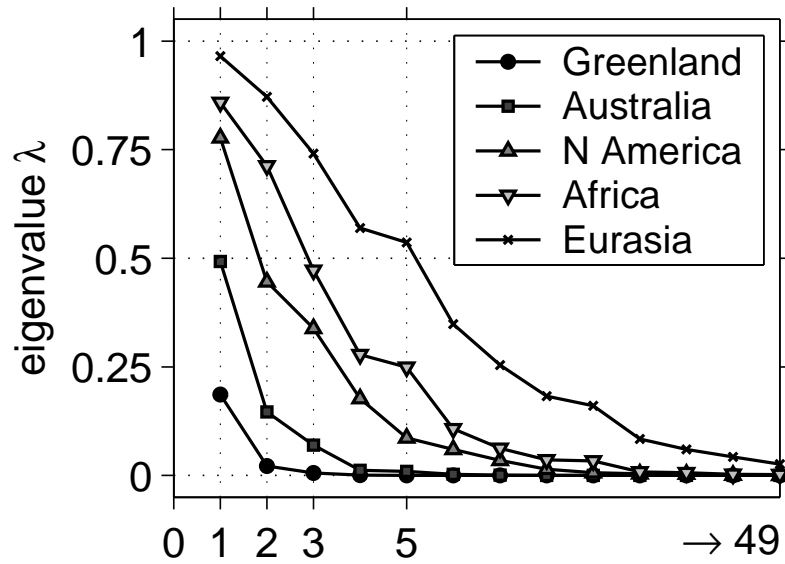
Diagonalization of the operator D, with elements

$$D_{lm,l'm'} = \int_R Y_{lm} Y_{l'm'} \, d\Omega, \tag{15}$$

is often hard and sometimes impossible.

Diagonalization of the operator D, with elements

$$D_{lm,l'm'} = \int_R Y_{lm} Y_{l'm'} \, d\Omega, \qquad (16)$$

is often hard and sometimes impossible.

But if R is **axisymmetric**, i.e. a **single polar cap** or a **double polar cap**, we can find the Slepian functions as the solutions to a **different** eigenvalue problem involving a *very simple* kernel with *very well-behaved* eigenvalues.
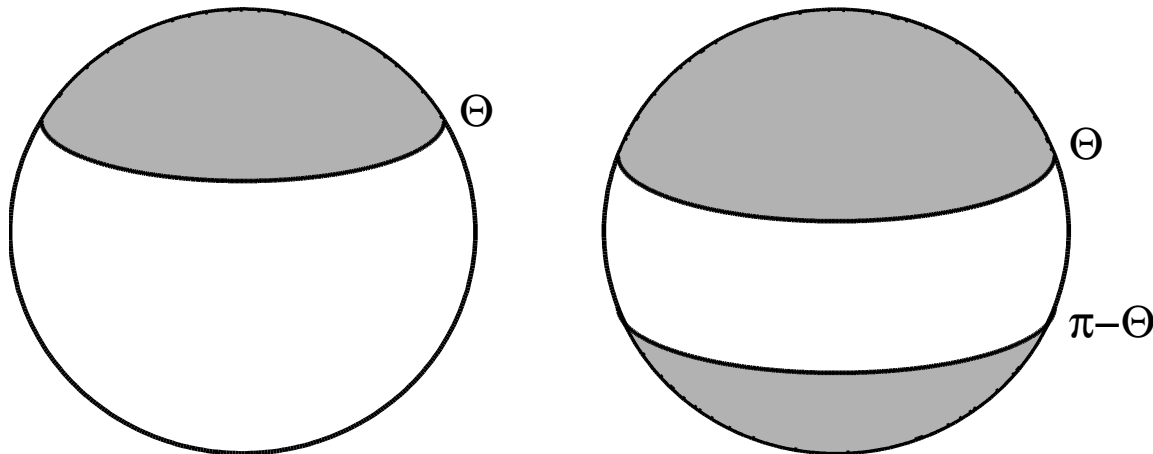
Summary of the theory (on the sphere)

Spherical harmonics Y_{lm} form an **orthonormal** basis on Ω:

$$\int_{\Omega} Y_{lm} Y_{l'm'} \, d\Omega = \delta_{ll'} \delta_{mm'}. \tag{17}$$

The spherical harmonics Y_{lm} are **not orthogonal** on R:

$$\int_{R} Y_{lm} Y_{l'm'} \, d\Omega = D_{lm,l'm'}. \tag{18}$$

Summary of the theory (on the sphere) — 1

Spherical harmonics Y_{lm} form an **orthonormal** basis on Ω:

$$\int_\Omega Y_{lm} Y_{l'm'} \, d\Omega = \delta_{ll'} \delta_{mm'}. \tag{17}$$

The spherical harmonics Y_{lm} are **not orthogonal** on R:

$$\int_R Y_{lm} Y_{l'm'} \, d\Omega = D_{lm,l'm'}. \tag{18}$$

The eigenfunctions of D are called **Slepian functions**, $g(\hat{\mathbf{r}})$. They form a **band-limited localized basis**, *doubly* orthogonal: on R (to λ) and *also* on Ω (to 1).

The **Shannon number**, or sum of the eigenvalues, the space-bandwidth product,

$$N = (L+1)^2 \frac{A}{4\pi},$$

is the **effective dimension** of the space for which the bandlimited g are a **basis**.

☑ Scalar fields

☐ Vector (potential) fields

☐ Tensor fields

☑ Scalar fields

☑ Vector (potential) fields

☐ Tensor fields

☑ Scalar fields

☑ Vector (potential) fields

☑ Tensor fields

The expansion of a bandlimited process on the sphere in *either* spherical harmonics or in Slepian functions is equal and *exact*:

$$s(\hat{\mathbf{r}}) = \sum_{l=0}^{L} \sum_{m=-l}^{l} s_{lm} Y_{lm}(\hat{\mathbf{r}}) = \sum_{\alpha=1}^{(L+1)^2} s_\alpha g_\alpha(\hat{\mathbf{r}}). \tag{19}$$

The expansion of a bandlimited process on the sphere in *either* spherical harmonics or in Slepian functions is equal and *exact*:

$$s(\hat{\mathbf{r}}) = \sum_{l=0}^{L} \sum_{m=-l}^{l} s_{lm} Y_{lm}(\hat{\mathbf{r}}) = \sum_{\alpha=1}^{(L+1)^2} s_{\alpha} g_{\alpha}(\hat{\mathbf{r}}). \tag{19}$$

But if the signal is **regional** in nature, an expansion into Slepian functions up until the Shannon number N will be **approximate but sparse**:

$$s(\hat{\mathbf{r}}) \approx \sum_{\alpha=1}^{N} s_{\alpha} g_{\alpha}(\hat{\mathbf{r}}), \qquad \hat{\mathbf{r}} \in R. \tag{20}$$

The *mean squared reconstruction error* in the noiseless case is determined by the neglected eigenvalues, which are **small** beyond the Shannon number N.

5040 (5027) spherical harmonic coefficients
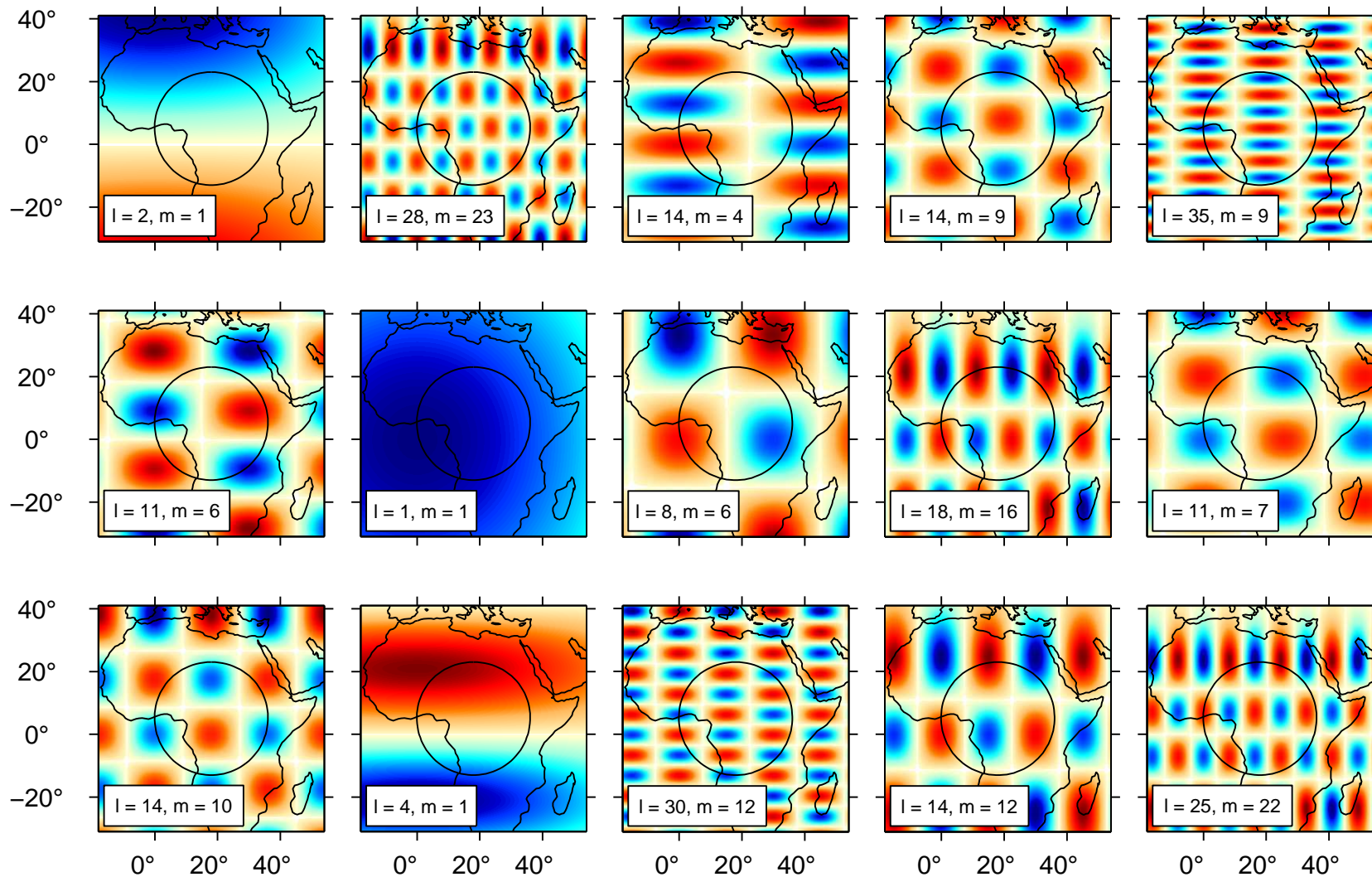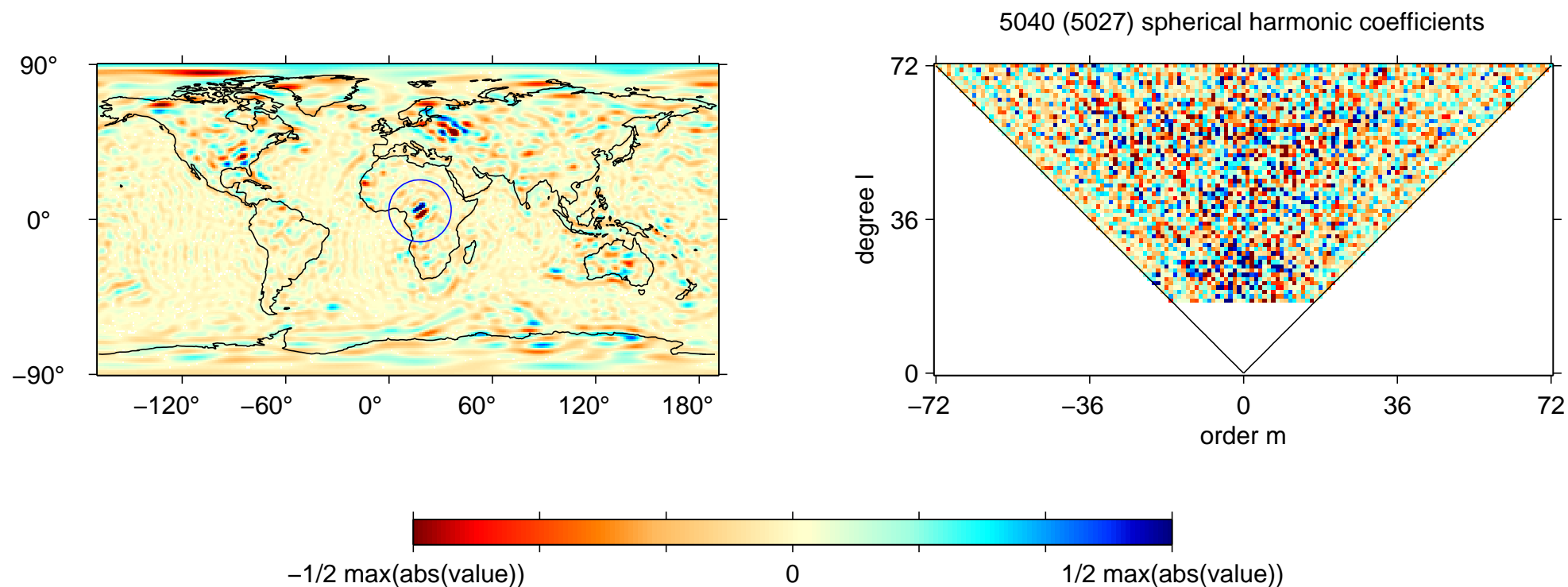
A *global* basis, **good** for *global* problems.

5329 (4181) spherical harmonic coefficients
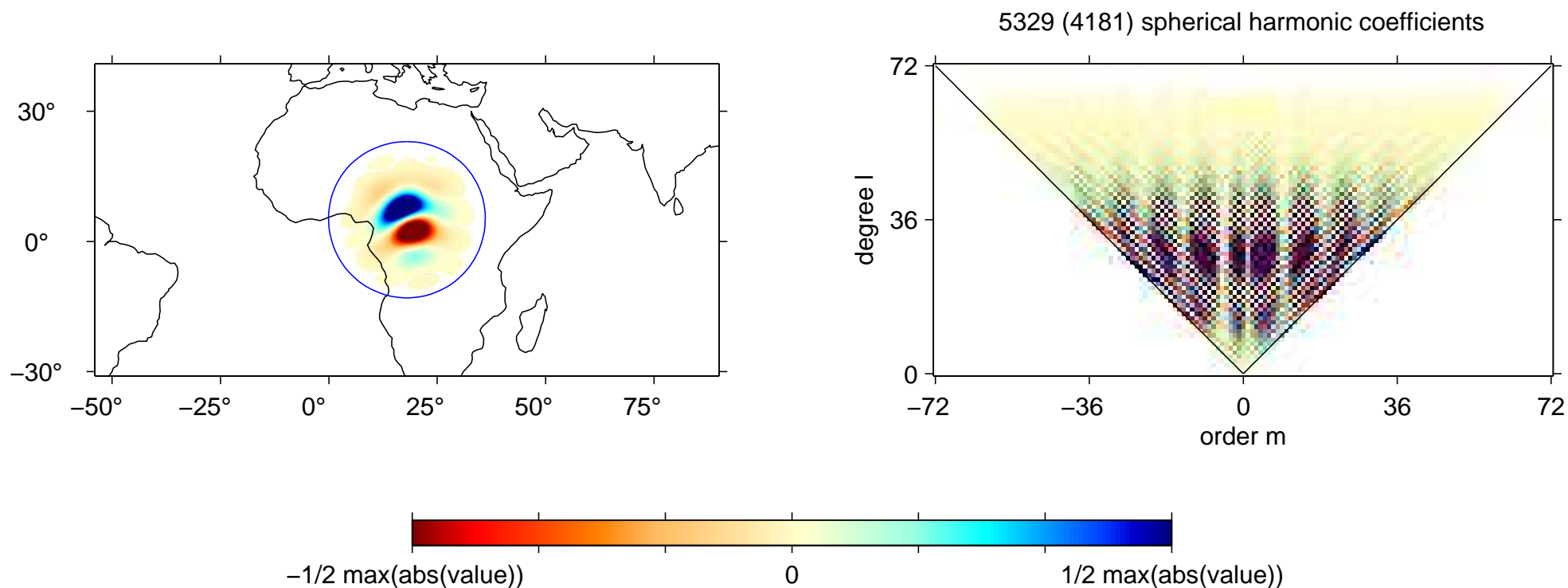
A *global* basis, **bad** for *local* problems.

An **orthogonal transform** by the eigenmatrix of D introduces welcome sparsity.

R−average mse 1.18e−09%

130 (41) Slepian coefficients
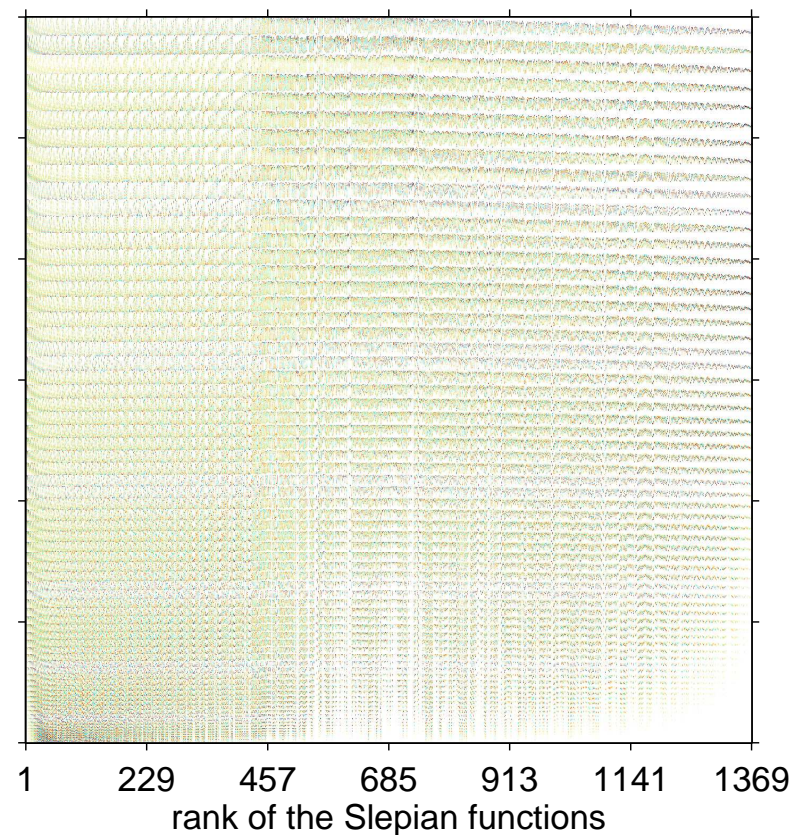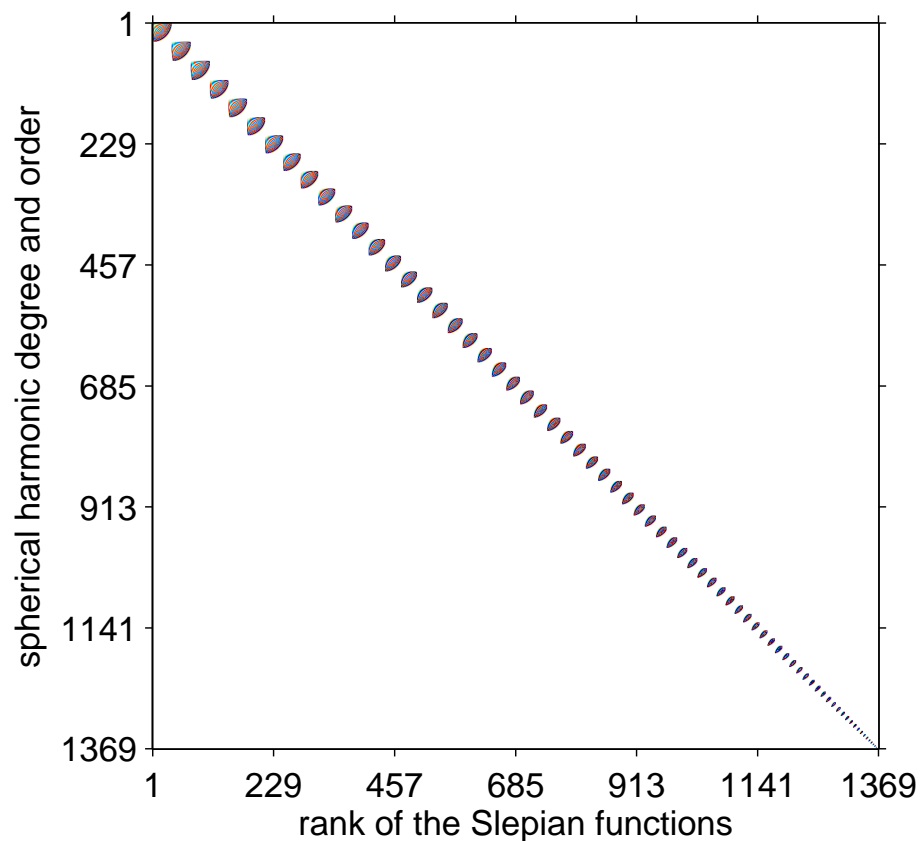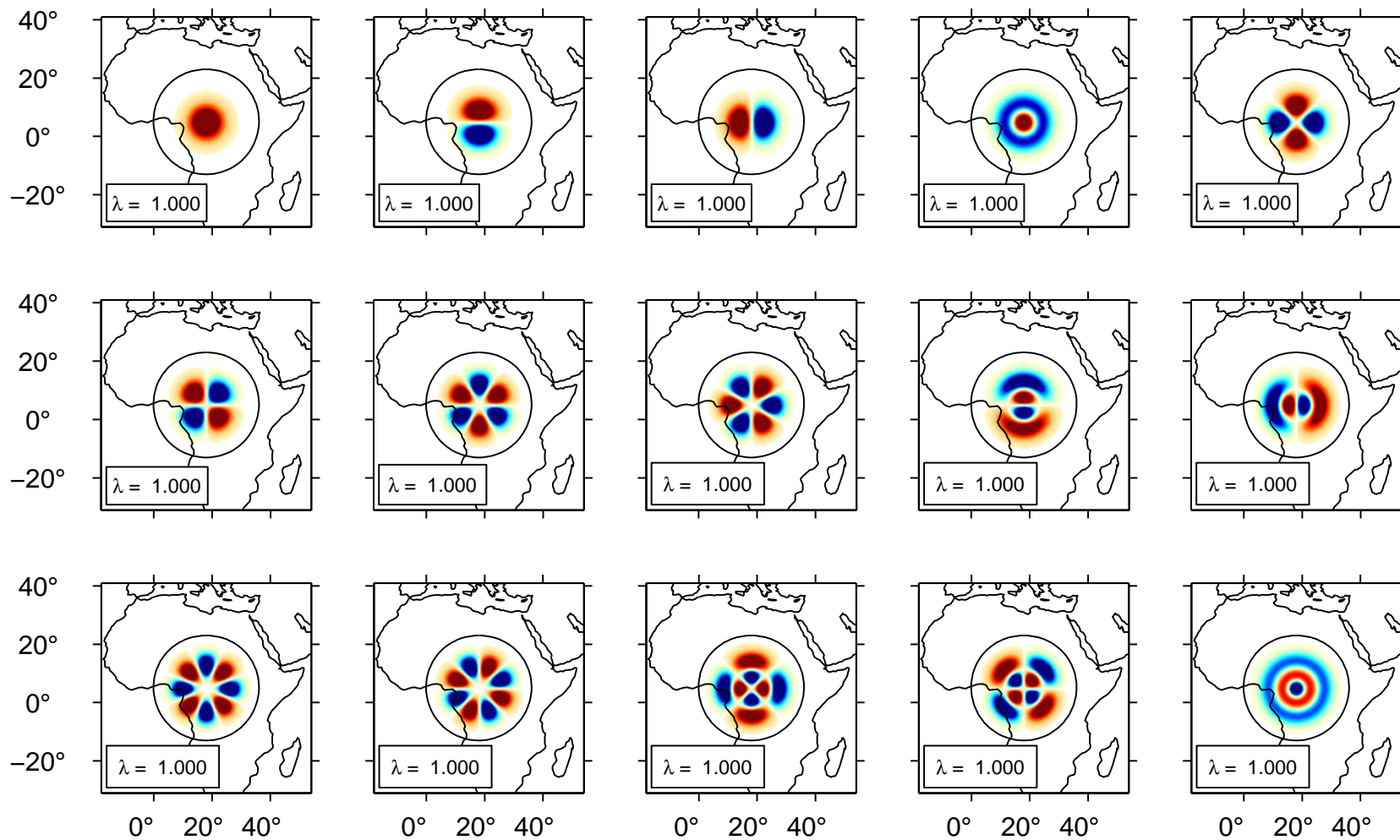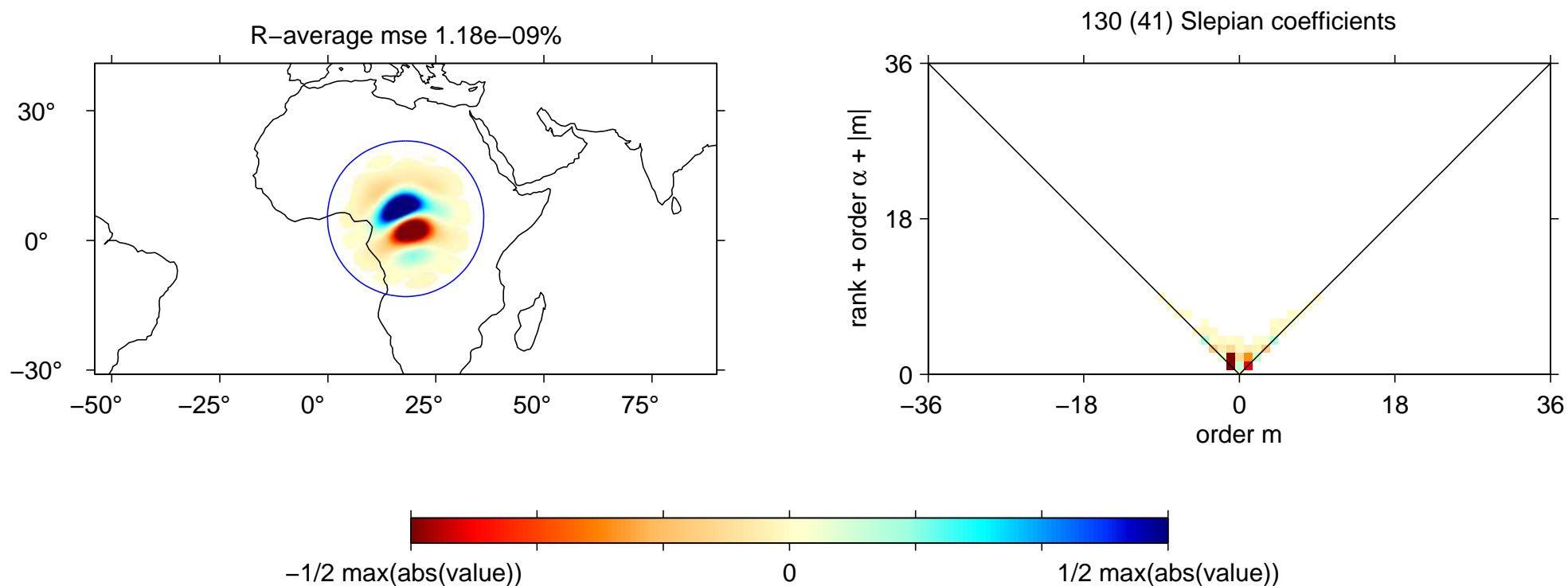
A *local* basis, **good** for *local* problems. Sparsity!

Earthquake "focal mechanisms" *look* like Slepian functions.
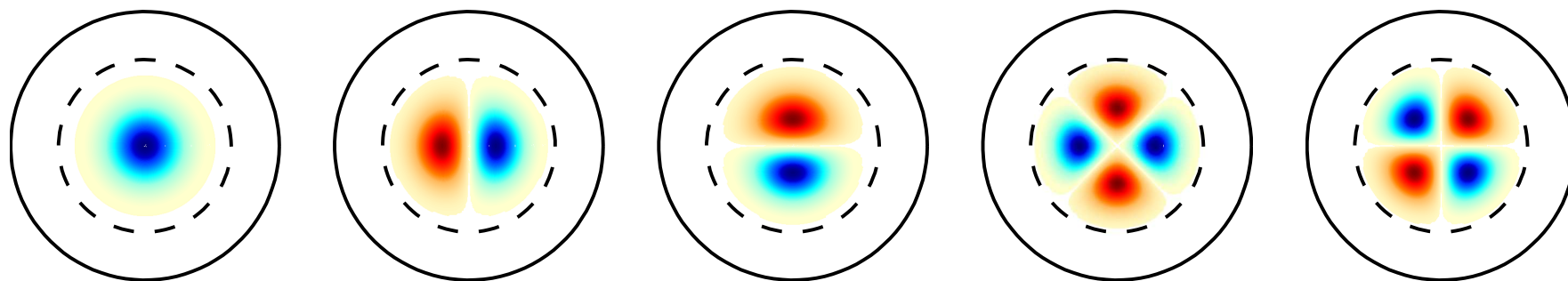
Example: using Slepian functions to unearth the signature of the great Sumatra-Andaman earthquake from GRACE **time-variable satellite gravity** data.

$\mathbf{M} = [1\ 0\ \text{-1}\ 0\ 0\ 0]/\sqrt{2}$ — $\mathbf{M} = [0\ 0\ 0\ 1\ 0\ 0]/\sqrt{2}$ — $\mathbf{M} = [0\ 1\ \text{-1}\ 0\ 0\ 0]/\sqrt{2}$

$\lambda_1 = 0.999944$ — $\lambda_2 = 0.998609$ — $\lambda_3 = 0.998609$
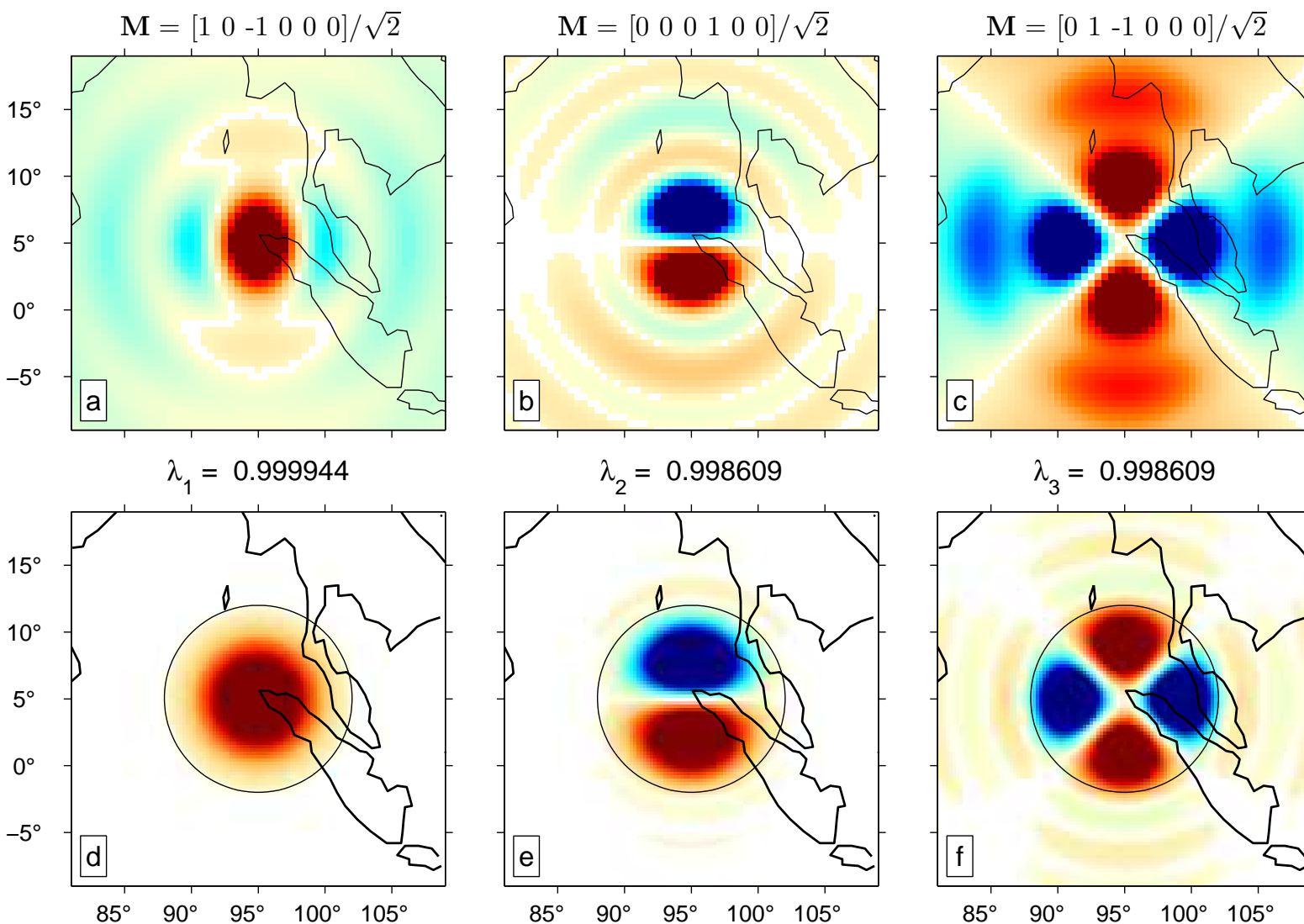
Application to the analysis of GRACE data

dGSM.2005.001.2005.031.0K20.geo

Geoid height variation [mm]

Application to the analysis of GRACE data
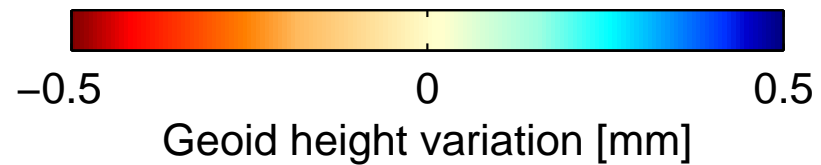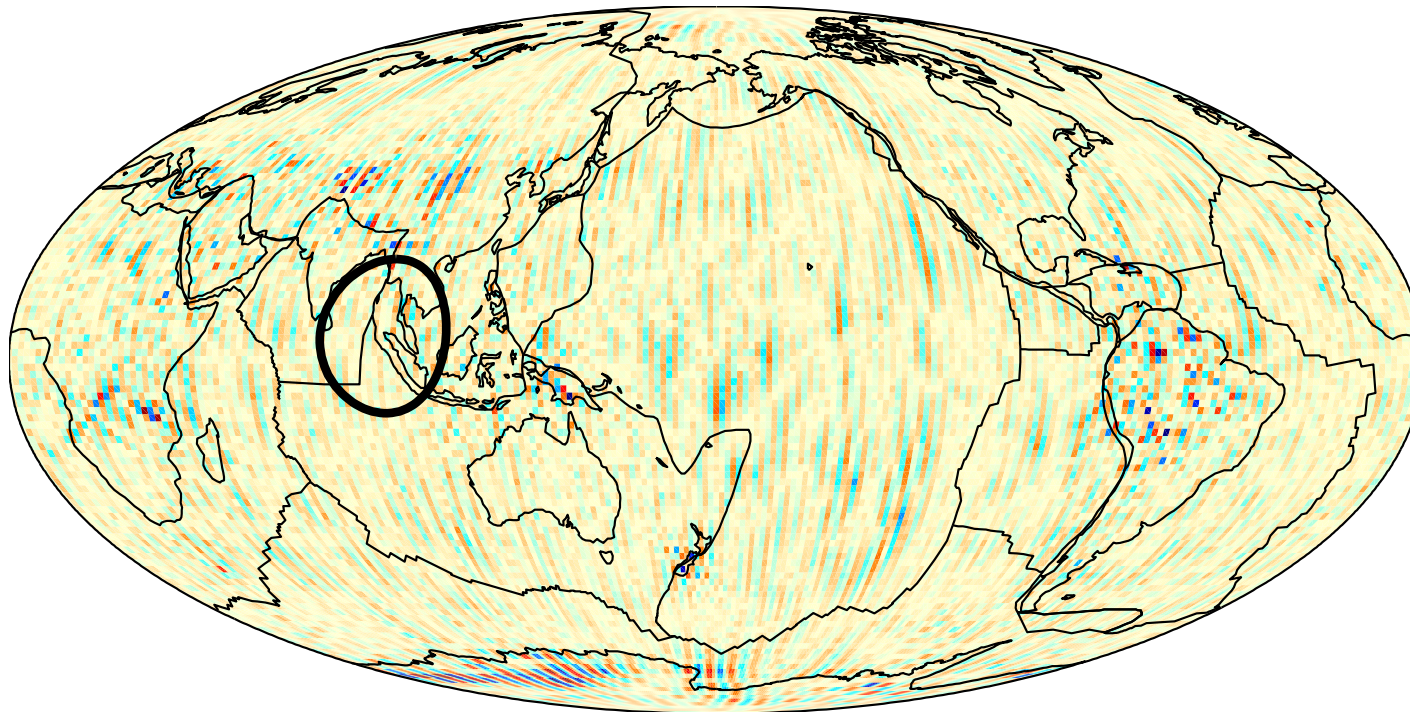
dGSM.2004.336.2004.366.0K20.geo
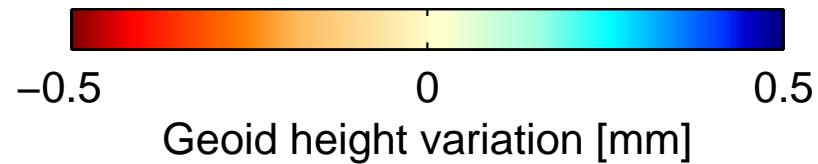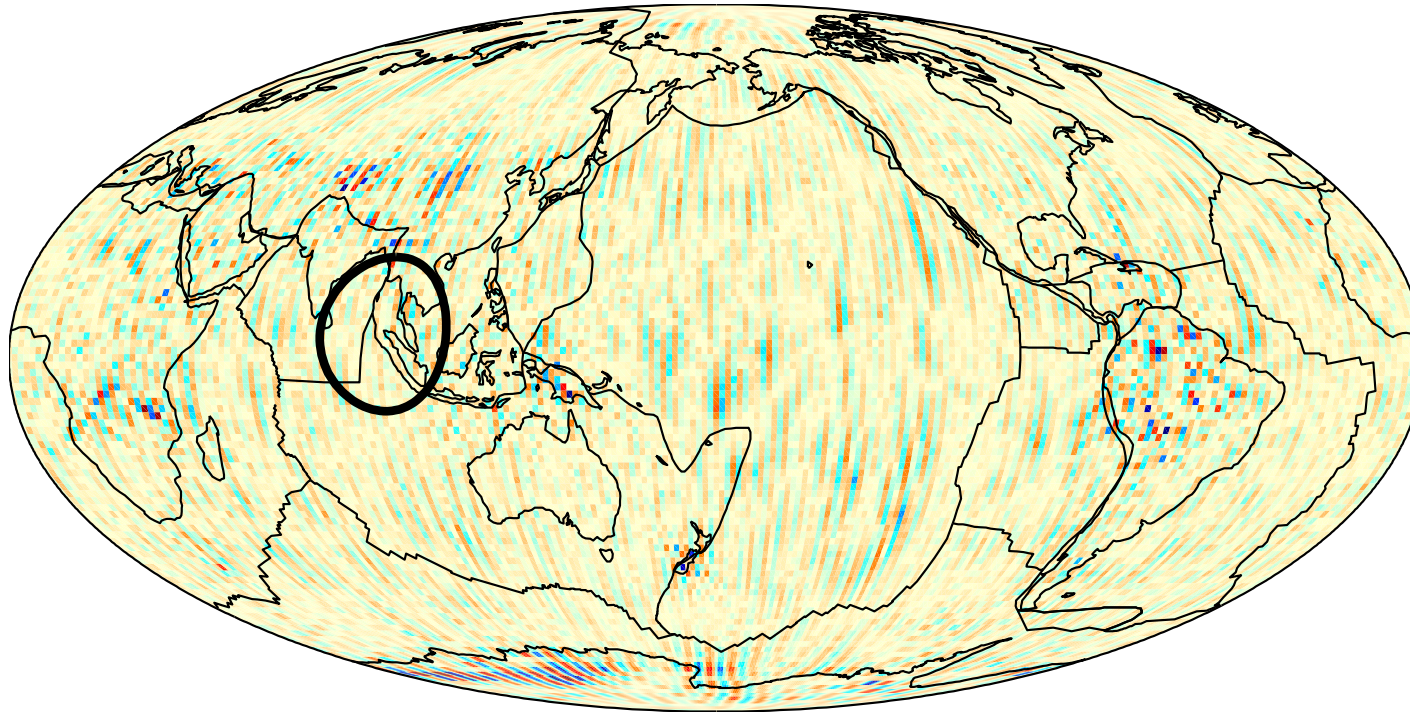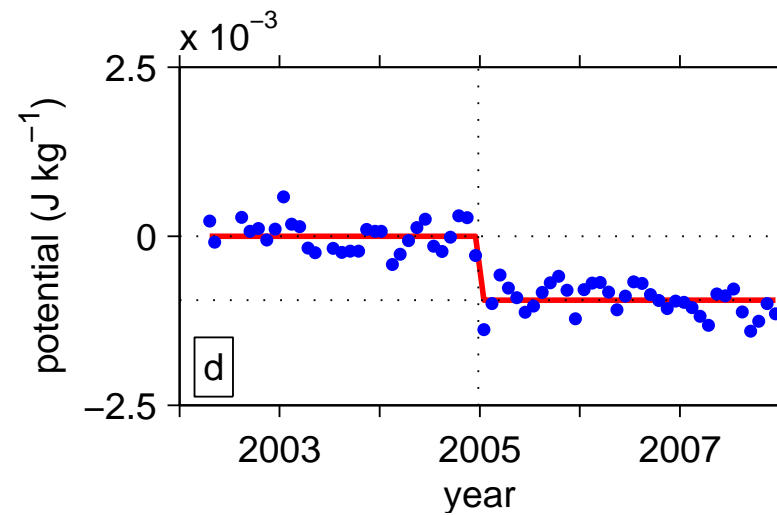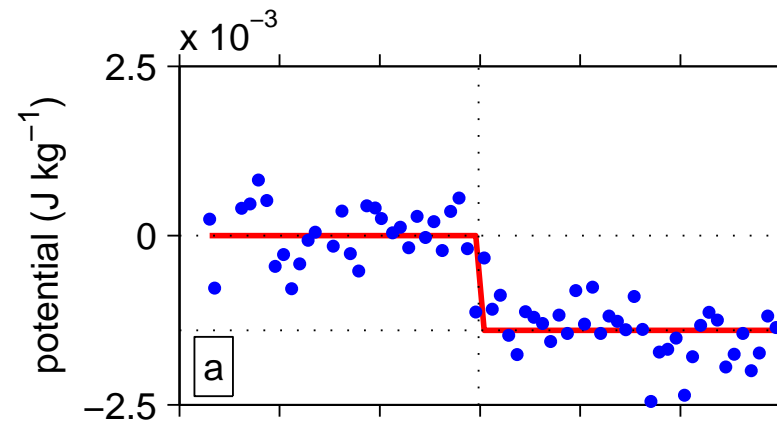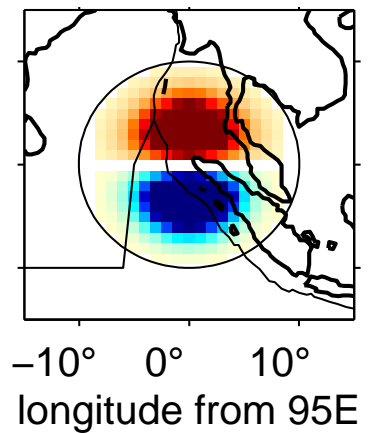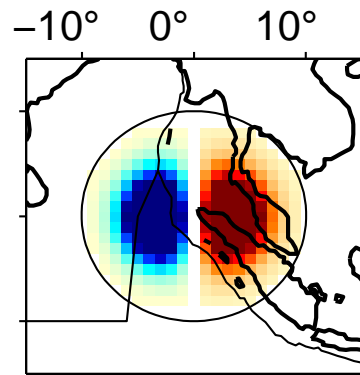
Geoid height variation [mm]

−0.5   0   0.5
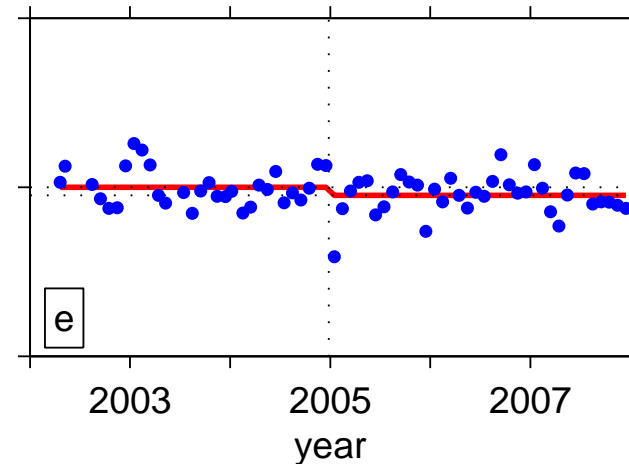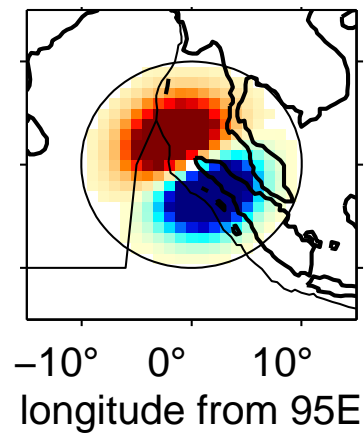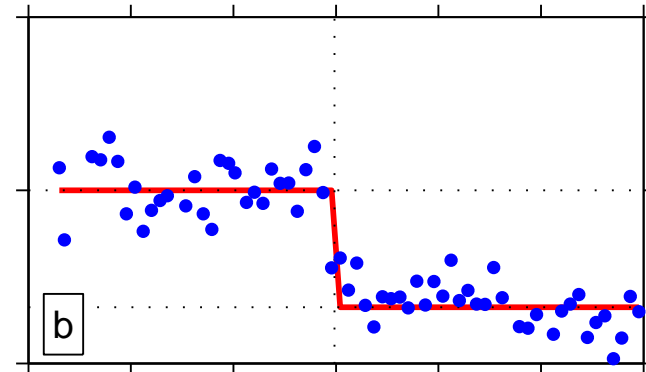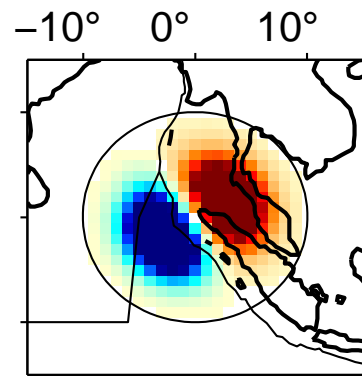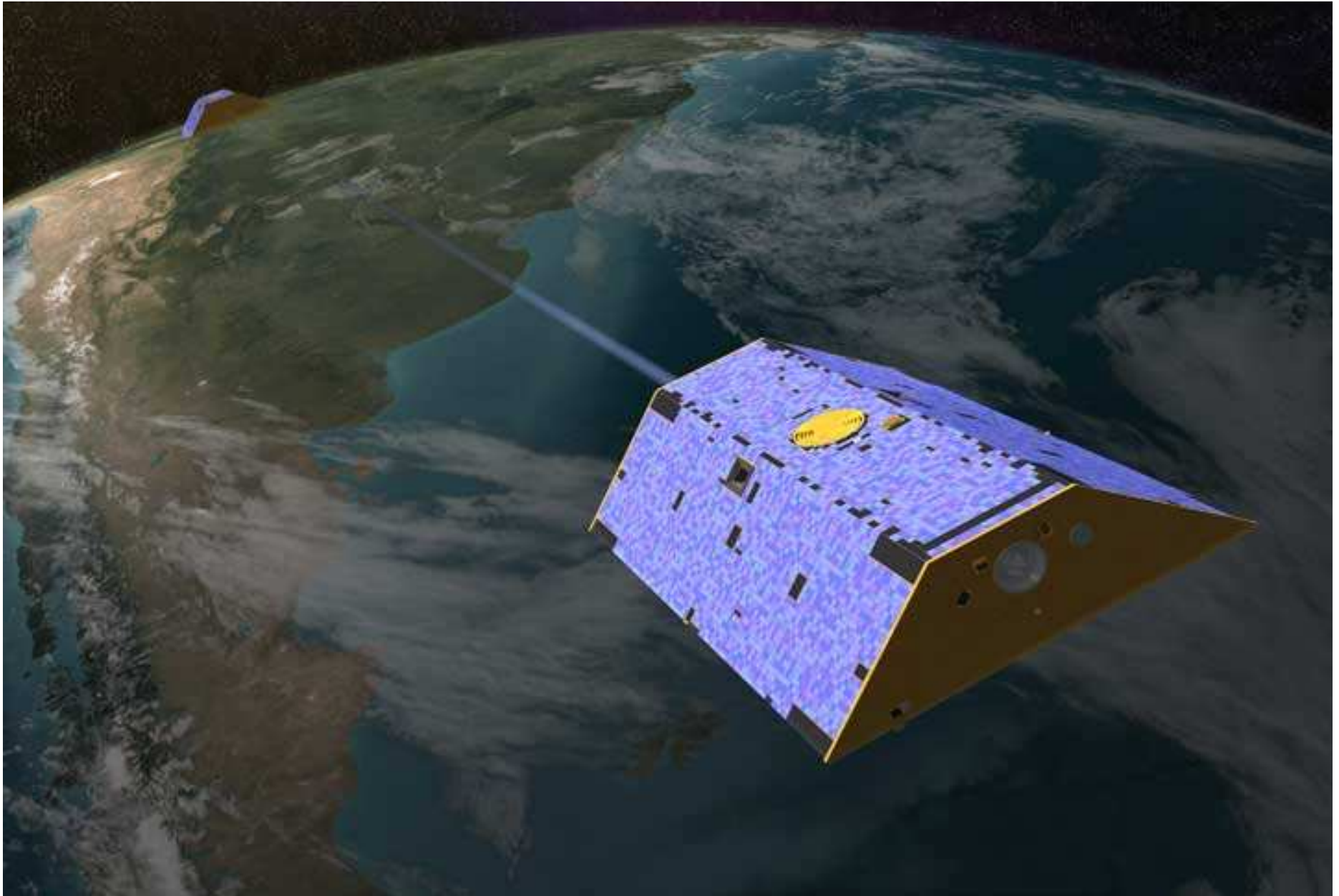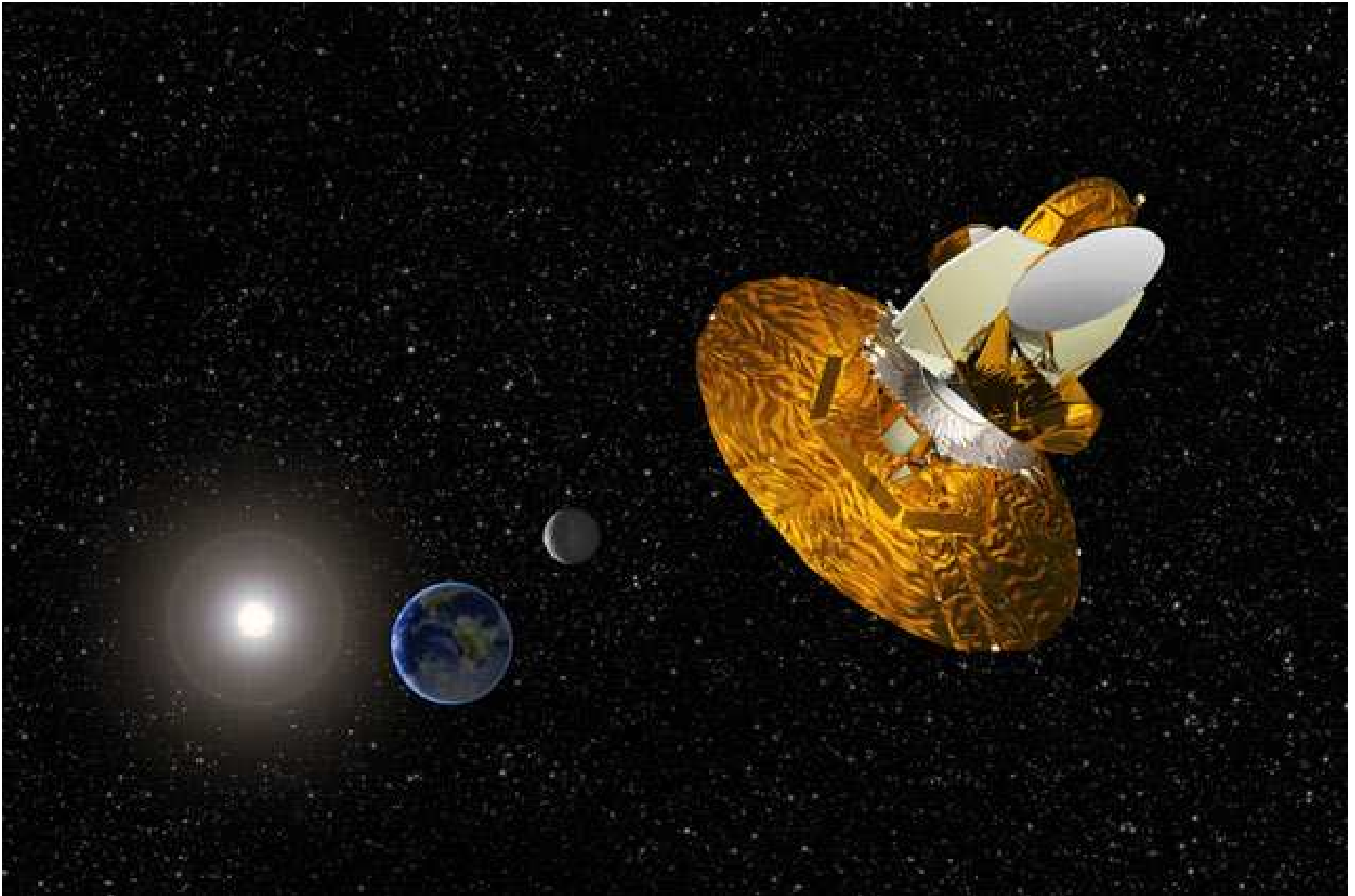
The data **collected in** or **limited to** R are **signal** plus **noise**:

We assume that $n(\mathbf{r})$ is **zero-mean** and **uncorrelated** with the signal

and consider known the **noise covariance**:

In other words: we've got **noisy** and **incomplete** data on the sphere.

The data **collected in** or **limited to** R are **signal** plus **noise**:

$$d(\mathbf{r}) = \begin{cases} s(\mathbf{r}) + n(\mathbf{r}) & \text{if } \mathbf{r} \in R, \\ \text{unknown/undesired} & \text{if } \mathbf{r} \in \Omega \setminus R. \end{cases}$$

We assume that $n(\mathbf{r})$ is **zero-mean** and **uncorrelated** with the signal

$$\langle n(\mathbf{r}) \rangle = 0 \quad \text{and} \quad \langle n(\mathbf{r}) s(\mathbf{r}') \rangle = 0,$$

and consider known the **noise covariance**:

$$\langle n(\mathbf{r}) n(\mathbf{r}') \rangle.$$

In other words: we've got **noisy** and **incomplete** data on the sphere.

dGSM.2005.001.2005.031.0K20.geo

Geoid height variation [mm]
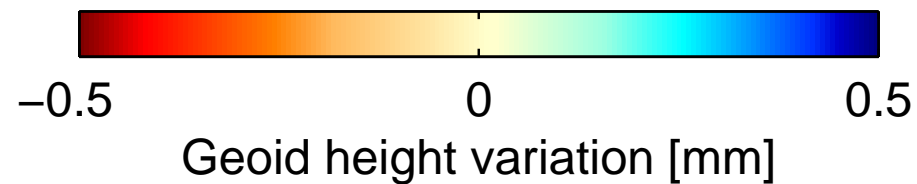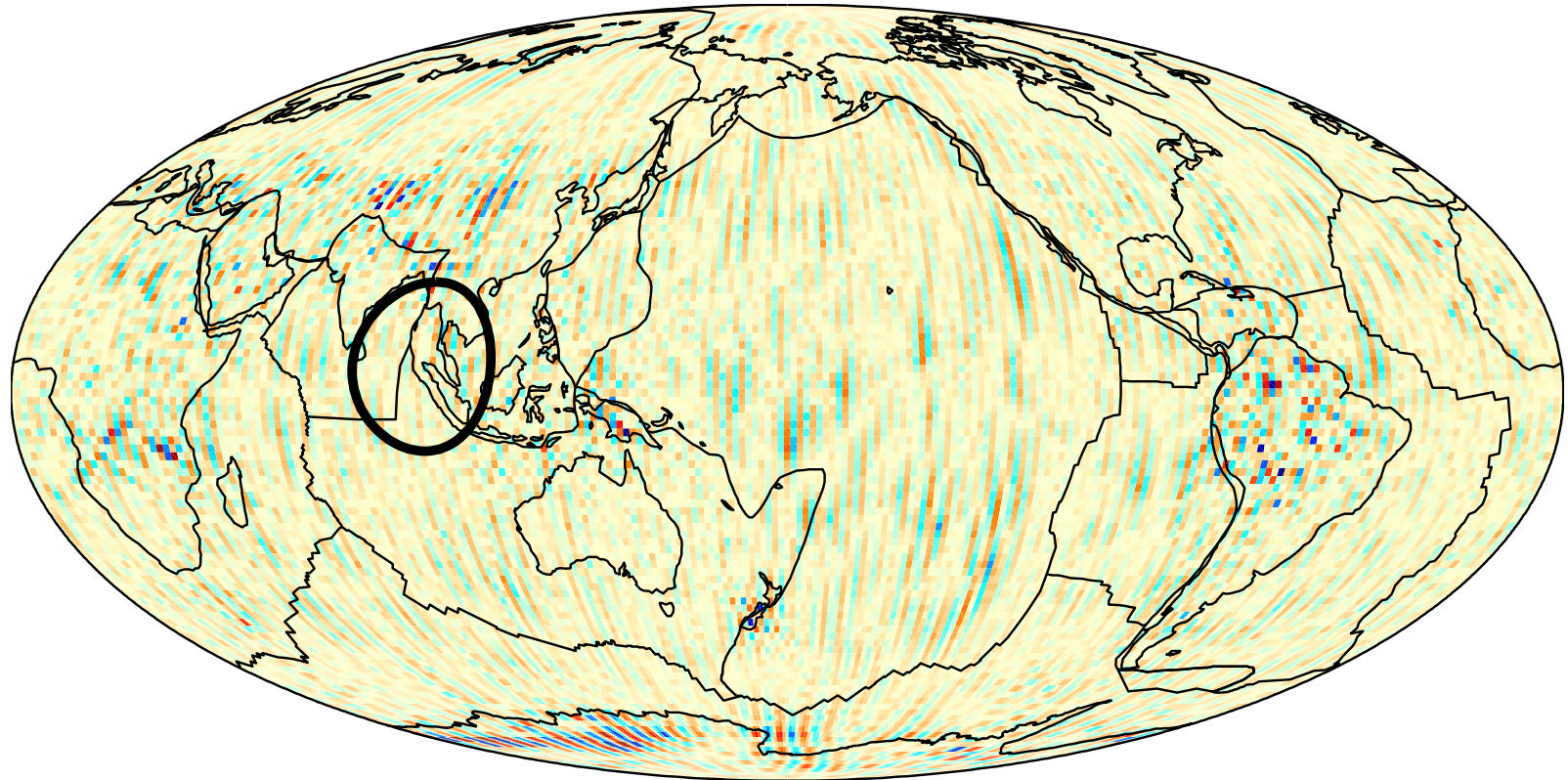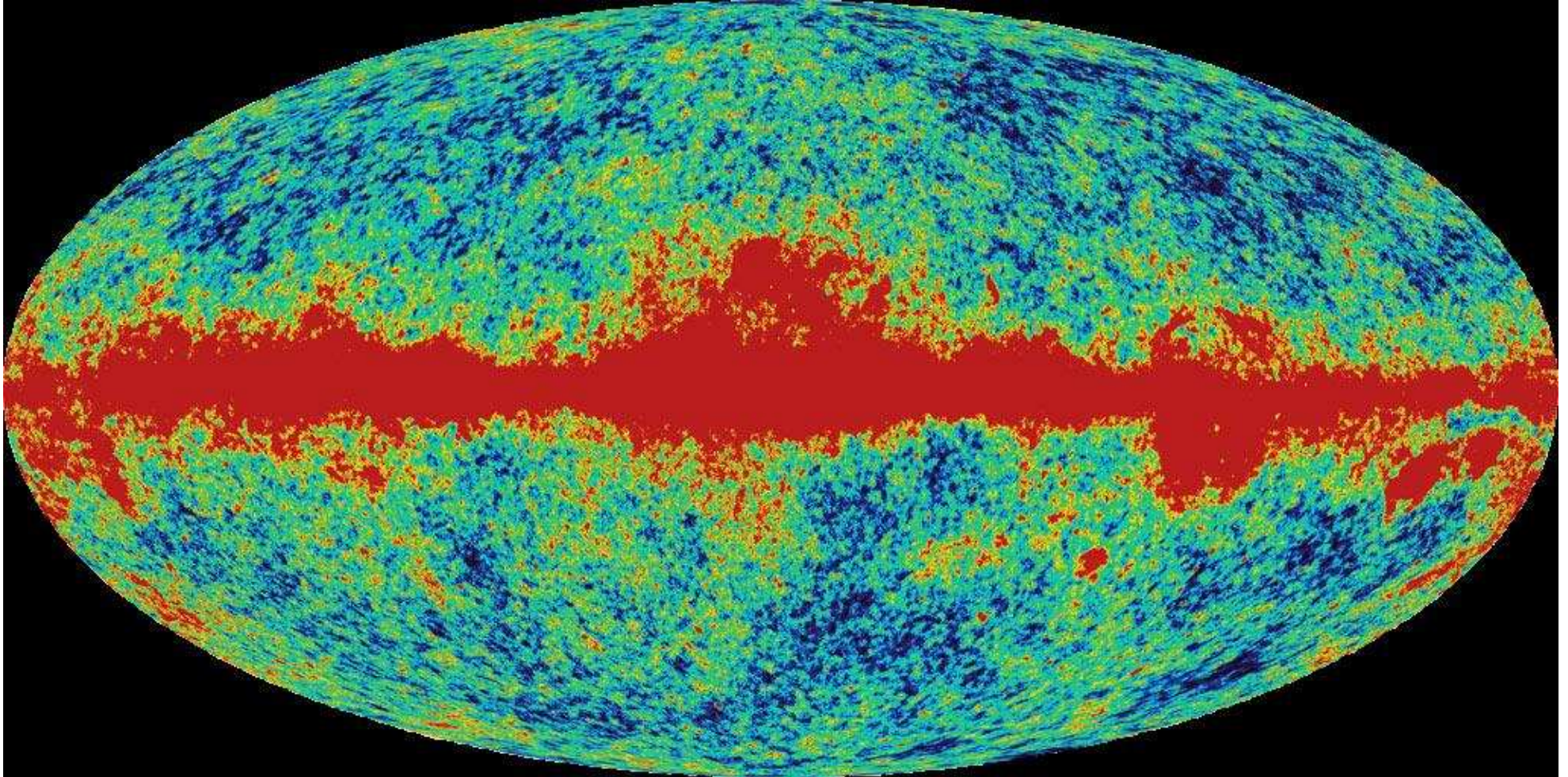
Consider an *unknown*, *noisily* and *incompletely observed* spherical process:

$$s(\mathbf{r}) = \sum_{lm}^{\infty} s_{lm} Y_{lm}(\mathbf{r}).$$

Linear Problem: **Problem 1**

Quadratic Problem: **Problem 2**

Consider an *unknown, noisily* and *incompletely observed* spherical process:

$$s(\mathbf{r}) = \sum_{lm}^{\infty} s_{lm} Y_{lm}(\mathbf{r}).$$

Linear Problem: **Problem 1**

Given $d(\mathbf{r})$ and $\langle n(\mathbf{r})n(\mathbf{r}')\rangle$, *estimate* the **signal** $s(\mathbf{r})$, realizing that the estimate $\hat{s}(\mathbf{r})$ is **always bandlimited** to $0 \leq L < \infty$.

Quadratic Problem: **Problem 2**

Consider an *unknown*, *noisily* and *incompletely observed* spherical process:

$$s(\mathbf{r}) = \sum_{lm}^{\infty} s_{lm} Y_{lm}(\mathbf{r}).$$

Linear Problem: **Problem 1**

> Given $d(\mathbf{r})$ and $\langle n(\mathbf{r})n(\mathbf{r}')\rangle$, *estimate* the **signal** $s(\mathbf{r})$, realizing that the estimate $\hat{s}(\mathbf{r})$ is **always bandlimited** to $0 \leq L < \infty$.

Quadratic Problem: **Problem 2**

> Given $d(\mathbf{r})$ and $\langle n(\mathbf{r})n(\mathbf{r}')\rangle$, and assuming the field behaves as
> $$\langle s_{lm}\rangle = 0 \quad \text{and} \quad \langle s_{lm}s_{l'm'}\rangle = S_l\,\delta_{ll'}\delta_{mm'},$$
> *estimate* the **power spectral density** S_l, for $0 \leq l < \infty$, as $\hat{S}_l$.

The data are **noisy** and **incomplete**.

The data are **noisy** and **incomplete**.

Problem 1

Find the **signal** that gives rise to the data.

The data are **noisy** and **incomplete**.

Problem 1

Find the **signal** that gives rise to the data.

Problem 2

Find the **power spectral density** of the signal.

Construct a **bandlimited estimate** in the spherical harmonic basis by minimizing the **misfit to the data** over R. The—*linear*—optimal solution depends on D^{-1}:

$$\hat{s}_{lm} = \sum_{l'm'}^{L} D_{lm,l'm'}^{-1} \int_{R} d\, Y_{l'm'} \, d\Omega.$$

Problem 1 — Finding the *signal*

Construct a **bandlimited estimate** in the spherical harmonic basis by minimizing the **misfit to the data** over R. The—*linear*—optimal solution depends on D^{-1}:

$$\hat{s}_{lm} = \sum_{l'm'}^{L} D^{-1}_{lm,l'm'} \int_R d\, Y_{l'm'} \, d\Omega.$$

Finding D^{-1} is tough, so construct a **truncated-Slepian basis** estimate instead:

$$\hat{s}(\mathbf{r}) = \sum_{\alpha}^{J} \hat{s}_\alpha g_\alpha(\mathbf{r}).$$

Problem 1 — Finding the *signal*

Construct a **bandlimited estimate** in the spherical harmonic basis by minimizing the **misfit to the data** over R. The—*linear*—optimal solution depends on D^{-1}:

$$\hat{s}_{lm} = \sum_{l'm'}^{L} D^{-1}_{lm,l'm'} \int_R d\, Y_{l'm'}\, d\Omega.$$

Finding D^{-1} is tough, so construct a **truncated-Slepian basis** estimate instead:

$$\boxed{\hat{s}(\mathbf{r}) = \sum_{\alpha}^{J} \hat{s}_{\alpha} g_{\alpha}(\mathbf{r}).}$$

The solution depends on the localization **eigenvalue at the same rank**:

$$\hat{s}_{\alpha} = \lambda_{\alpha}^{-1} \int_R d\, g_{\alpha}\, d\Omega.$$

b) 1/2003 – 6/2014

Int=−2312

surface density change (cm w.e.)
−200 −100 0 100 200

c) CSR–RL05

Ice Mass (Gt)

Slope = −243 ± 11 Gt/yr
Acceleration = −17 ± 7 Gt/yr^2

Time

1/2003–1/2013

Int=−1083

surface density change (cm water equivalent)

a) West Antarctica

Slope = −124 ± 3 Gt/yr
Acceleration = −27 ± 2 Gt/yr^2

If we simply worked with the available data we'd be using a **boxcar** window:

$$\hat{S}_l^{\mathrm{SP}} = \frac{1}{2l+1} \sum_m \left| \int_R d(\mathbf{r})\, Y_{lm}(\mathbf{r})\, d\Omega \right|^2.$$

If we simply worked with the available data we'd be using a **boxcar** window:

$$\hat{S}_l^{\mathrm{SP}} = \frac{1}{2l+1} \sum_m \left| \int_R d(\mathbf{r})\, Y_{lm}(\mathbf{r})\, d\Omega \right|^2 .$$

This estimate is **biased** (unless $S_l = S$ or $R = \Omega$), *coupling* over the *entire* band.

Its **bias**, **variance**, and thus **mean-squared error** depend, again, on D:

$$\mathrm{mse}_l^{\mathrm{SP}} \sim \sum_{mm'} \left| D_{lm,lm'} \right|^2 .$$

If we simply worked with the available data we'd be using a **boxcar** window:

$$\hat{S}_l^{\text{SP}} = \frac{1}{2l+1} \sum_m \left| \int_R d(\mathbf{r}) \, Y_{lm}(\mathbf{r}) \, d\Omega \right|^2.$$

This estimate is **biased** (unless $S_l = S$ or $R = \Omega$), *coupling* over the *entire* band.

Its **bias**, **variance**, and thus **mean-squared error** depend, again, on D:

$$\text{mse}_l^{\text{SP}} \sim \sum_{mm'} \left| D_{lm,lm'} \right|^2.$$

The **multitaper estimate** uses a *small* L for the Slepian windows $g_\alpha(\mathbf{r})$ over R,

$$\hat{S}_l^{\text{MT}} = \sum_\alpha \lambda_\alpha \left(\frac{1}{2l+1} \sum_m \left| \int_\Omega g_\alpha(\mathbf{r}) \, d(\mathbf{r}) \, Y_{lm}(\mathbf{r}) \, d\Omega \right|^2 \right).$$

Maximum-likelihood *... very cumbersome, unbiased, high variance*

Maximum-likelihood *... very cumbersome, unbiased, high variance*

Whole-sphere *... unattainable*

$$\hat{S}_l^{\mathrm{WS}} = \frac{1}{2l+1} \sum_m \left| \int_\Omega d(\mathbf{r})\, Y_{lm}^*(\mathbf{r})\, d\Omega \right|^2 - \text{noise correction.} \qquad (14)$$

Maximum-likelihood ... *very cumbersome, unbiased, high variance*

Whole-sphere ... *unattainable*

$$\hat{S}_l^{\mathrm{WS}} = \frac{1}{2l+1} \sum_m \left| \int_\Omega d(\mathbf{r}) \, Y_{lm}^*(\mathbf{r}) \, d\Omega \right|^2 - \text{noise correction.} \tag{14}$$

Periodogram ... *broadband bias, high variance*

$$\hat{S}_l^{\mathrm{SP}} = \left(\frac{4\pi}{A}\right) \frac{1}{2l+1} \sum_m \left| \int_R d(\mathbf{r}) \, Y_{lm}^*(\mathbf{r}) \, d\Omega \right|^2 - \text{noise correction.} \tag{15}$$

Maximum-likelihood *... very cumbersome, unbiased, high variance*

Whole-sphere *... unattainable*

$$\hat{S}_l^{\mathrm{WS}} = \frac{1}{2l+1} \sum_m \left| \int_\Omega d(\mathbf{r})\, Y_{lm}^*(\mathbf{r})\, d\Omega \right|^2 - \text{noise correction.} \qquad (14)$$

Periodogram *... broadband bias, high variance*

$$\hat{S}_l^{\mathrm{SP}} = \left(\frac{4\pi}{A}\right) \frac{1}{2l+1} \sum_m \left| \int_R d(\mathbf{r})\, Y_{lm}^*(\mathbf{r})\, d\Omega \right|^2 - \text{noise correction.} \quad (15)$$

Single-taper *... bandlimited bias*

$$\hat{S}_l^{\alpha} = \frac{1}{2l+1} \sum_m \left| \int_\Omega g_\alpha(\mathbf{r})\, d(\mathbf{r})\, Y_{lm}^*(\mathbf{r})\, d\Omega \right|^2 - \text{noise correction.} \quad (16)$$

Maximum-likelihood *... very cumbersome, unbiased, high variance*

Whole-sphere *... unattainable*

$$\hat{S}_l^{\mathrm{WS}} = \frac{1}{2l+1} \sum_m \left| \int_\Omega d(\mathbf{r})\, Y_{lm}^*(\mathbf{r})\, d\Omega \right|^2 - \text{noise correction.} \qquad (14)$$

Periodogram *... broadband bias, high variance*

$$\hat{S}_l^{\mathrm{SP}} = \left(\frac{4\pi}{A} \right) \frac{1}{2l+1} \sum_m \left| \int_R d(\mathbf{r})\, Y_{lm}^*(\mathbf{r})\, d\Omega \right|^2 - \text{noise correction.} \qquad (15)$$

Single-taper *... bandlimited bias*

$$\hat{S}_l^\alpha = \frac{1}{2l+1} \sum_m \left| \int_\Omega g_\alpha(\mathbf{r})\, d(\mathbf{r})\, Y_{lm}^*(\mathbf{r})\, d\Omega \right|^2 - \text{noise correction.} \qquad (16)$$

Multiple-taper *... bandlimited bias, lower variance, easily implemented*

$$\hat{S}_l^{\mathrm{MT}} = \frac{1}{K} \sum_\alpha \lambda_\alpha \hat{S}_l^\alpha. \qquad (17)$$

The *multitaper* method

It returns a **spectrally bandlimited** (to $\pm L$) average of the true spectral power while being sensitive to a **spatially localized** patch R of data.

Spectral and spatial concentration trade off via the **Shannon number**, which is the sole parameter to be chosen by the analyst:

$$N = (L + 1)^2 \frac{A}{4\pi}.$$

The *multitaper* method

It returns a **spectrally bandlimited** (to $\pm L$) average of the true spectral power while being sensitive to a **spatially localized** patch R of data.

Spectral and spatial concentration trade off via the **Shannon number**, which is the sole parameter to be chosen by the analyst:

$$N = (L + 1)^2 \frac{A}{4\pi}.$$

This dictates the deliberate **bias** of the estimate. More tapers $\rightarrow$ more bias, but the **covariance** matrix of the estimates *between* tapers is almost **diagonal**.

The *multitaper* method

It returns a **spectrally bandlimited** (to $\pm L$) average of the true spectral power while being sensitive to a **spatially localized** patch R of data.

Spectral and spatial concentration trade off via the **Shannon number**, which is the sole parameter to be chosen by the analyst:

$$N = (L+1)^2 \frac{A}{4\pi}.$$

This dictates the deliberate **bias** of the estimate. More tapers $\rightarrow$ more bias, but the **covariance** matrix of the estimates *between* tapers is almost **diagonal**.

Thus, **weighted averaging** of estimates made with many different tapers **reduces the estimation variance**. And with *eigenvalue weighting*, the bias is strictly limited to the bandwidth L, and **independent of the shape** of the region R.
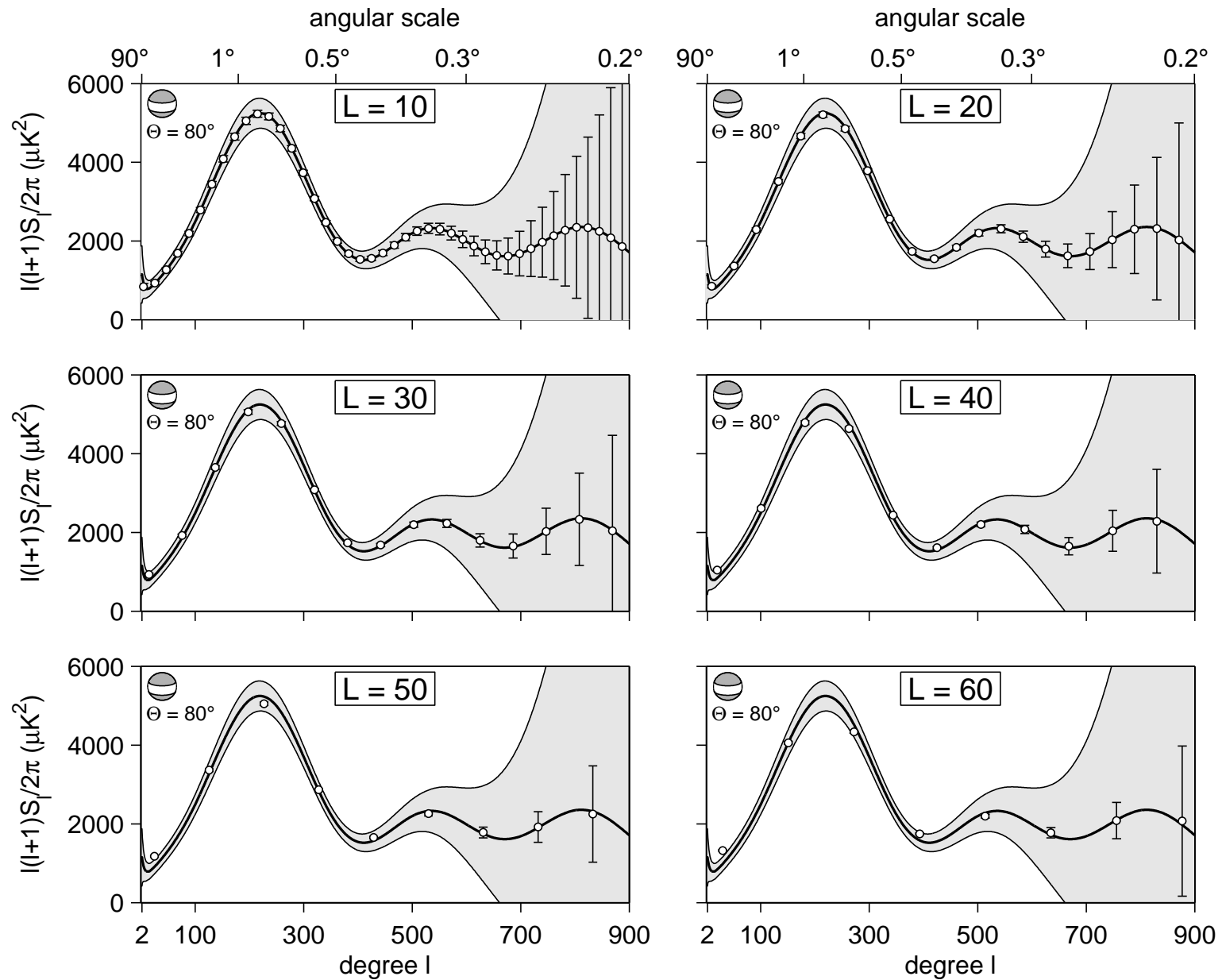
Using the choice of the **eigenvalues** λ of D as weights of the multitaper spectral estimate, the **multitaper coupling matrix** is

$$K_{ll'} = \frac{2l'+1}{(L+1)^2} \sum_{p}^{L} (2p+1) \begin{pmatrix} l & p & l' \\ 0 & 0 & 0 \end{pmatrix}^2,$$

which — amazingly — depends only upon the chosen bandwidth L.
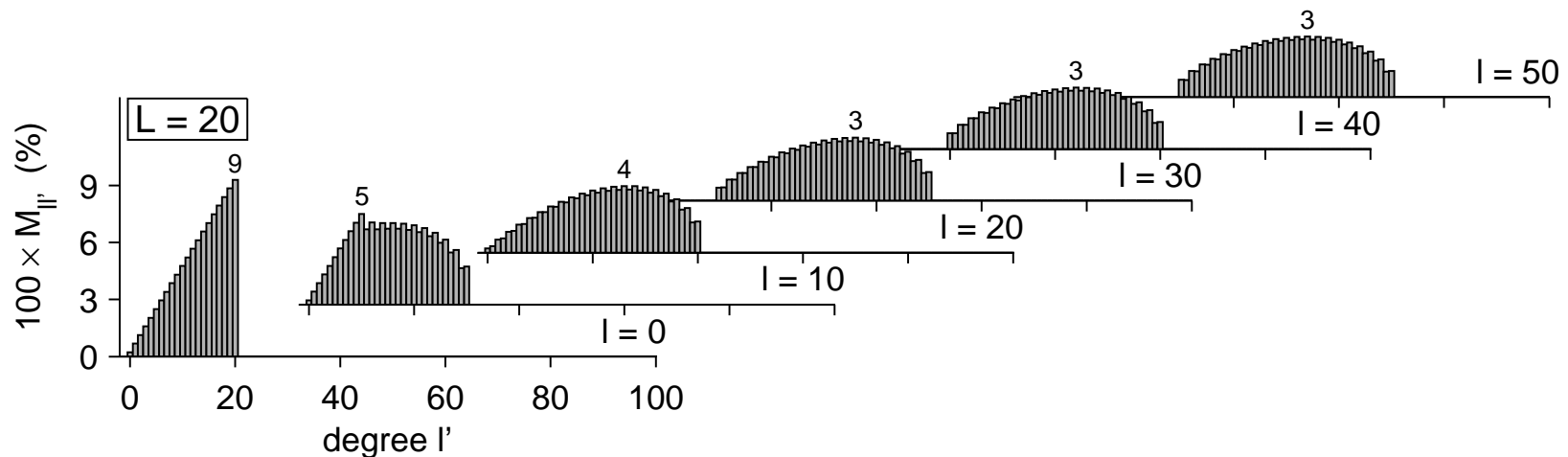
The **covariance** between the multitaper estimates is relatively simple when the spectra is **moderately colored** (compared to the bandwidth L of the estimator):

$$\Sigma_{ll'}^{\mathrm{MT}} = \frac{1}{2\pi}(S_l + N_l)(S_{l'} + N_{l'}) \sum_p (2p+1)\, \Gamma_p \begin{pmatrix} l & p & l' \\ 0 & 0 & 0 \end{pmatrix}^2, \quad (17)$$

$$\begin{aligned}
\Gamma_p \;\; = \;\; & \frac{1}{K^2} \sum_{ss'}^{L} \sum_{uu'}^{L} (2s+1)(2s'+1)(2u+1)(2u'+1) \sum_{e}^{2L} (-1)^{p+e}(2e+1)B_e \\
& \times \begin{Bmatrix} s & e & s' \\ u & p & u' \end{Bmatrix} \begin{pmatrix} s & e & s' \\ 0 & 0 & 0 \end{pmatrix} \begin{pmatrix} u & e & u' \\ 0 & 0 & 0 \end{pmatrix} \begin{pmatrix} s & p & u' \\ 0 & 0 & 0 \end{pmatrix} \begin{pmatrix} u & p & s' \\ 0 & 0 & 0 \end{pmatrix}, \quad (18)
\end{aligned}$$

with B_e the boxcar power, which depends on the **shape** of the region of interest, and the sums over angular degrees are limited by Wigner 3-j selection rules. The term in curly braces is a Wigner 6-j symbol. Ugly, but computable.
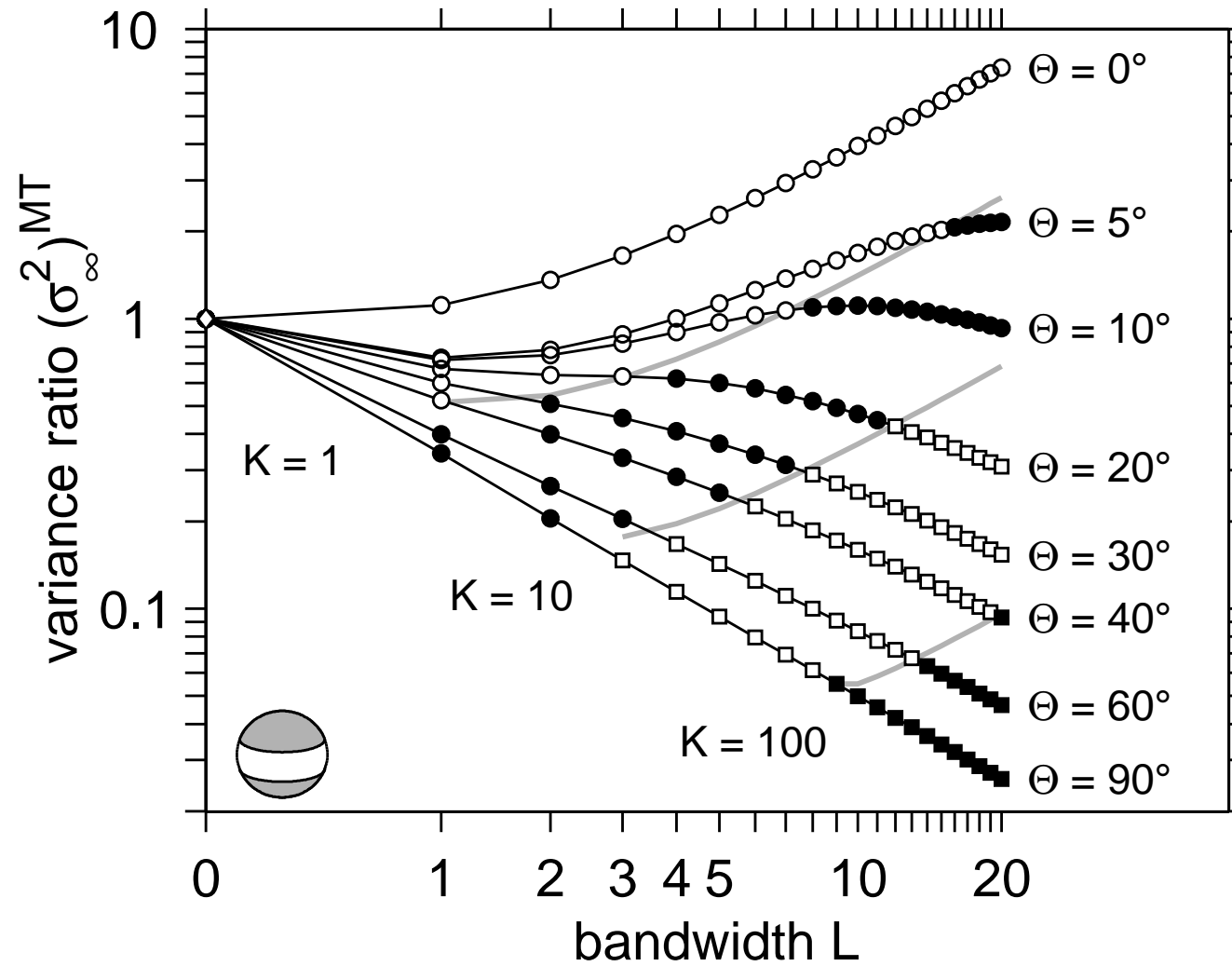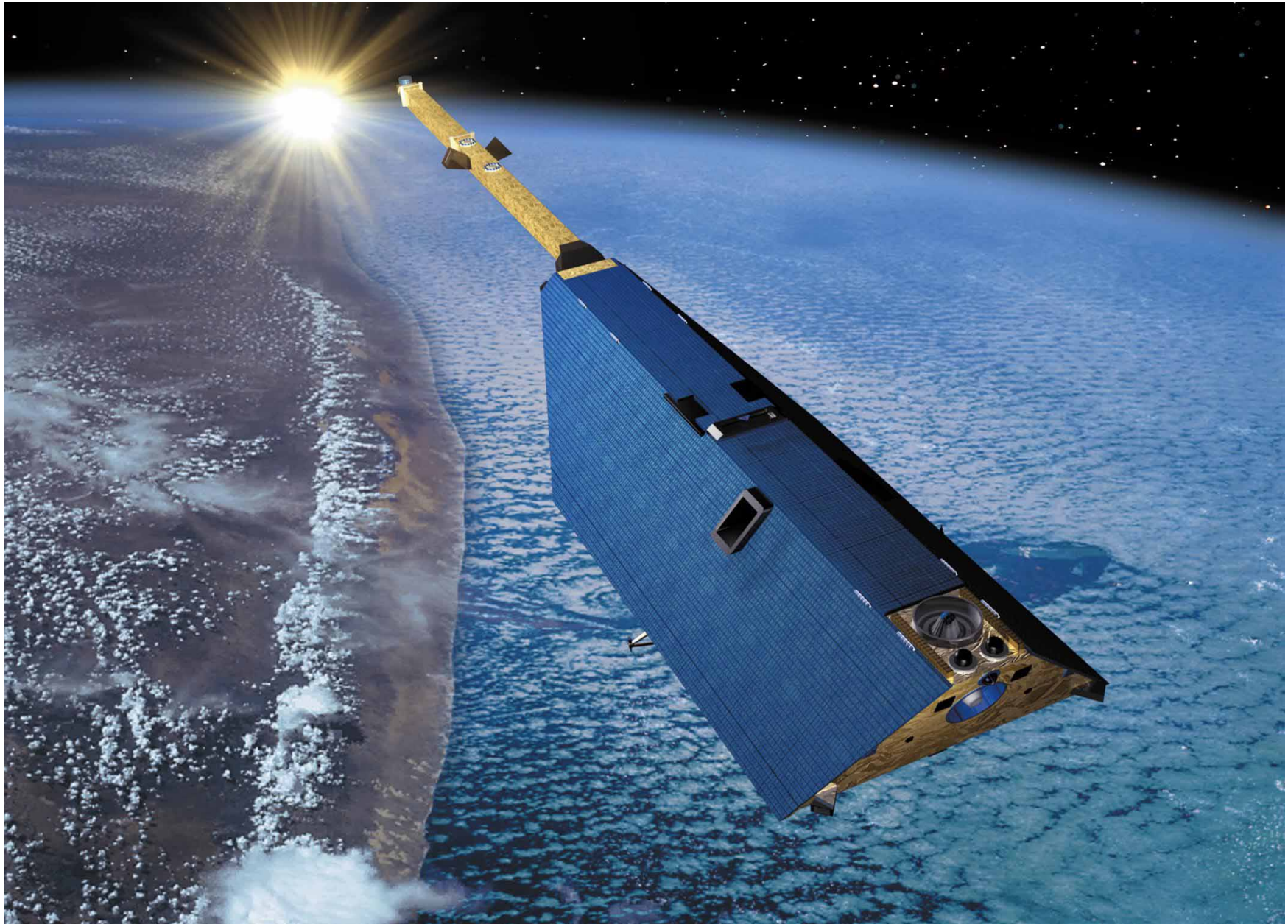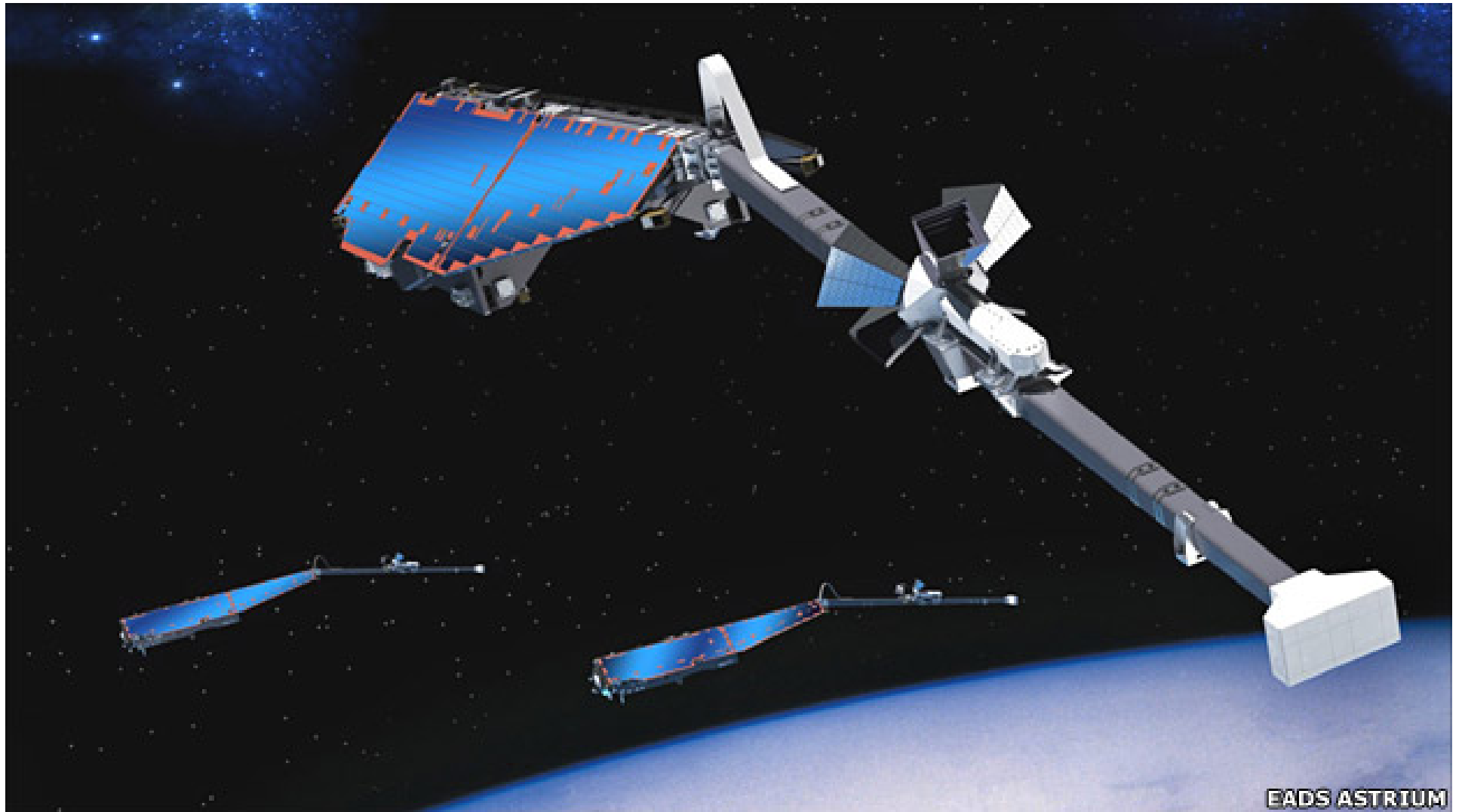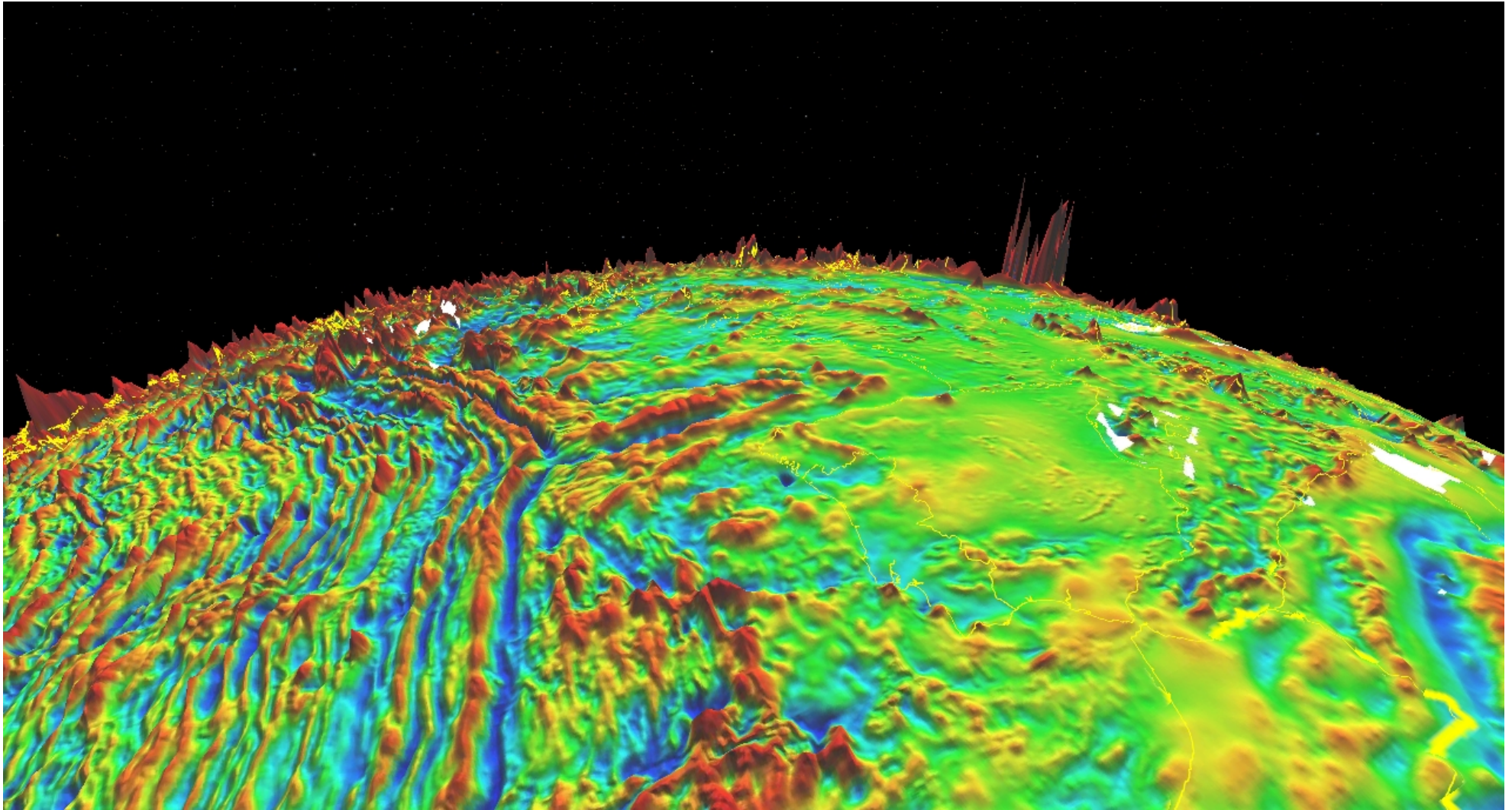
EADS ASTRIUM

(a)

(b)
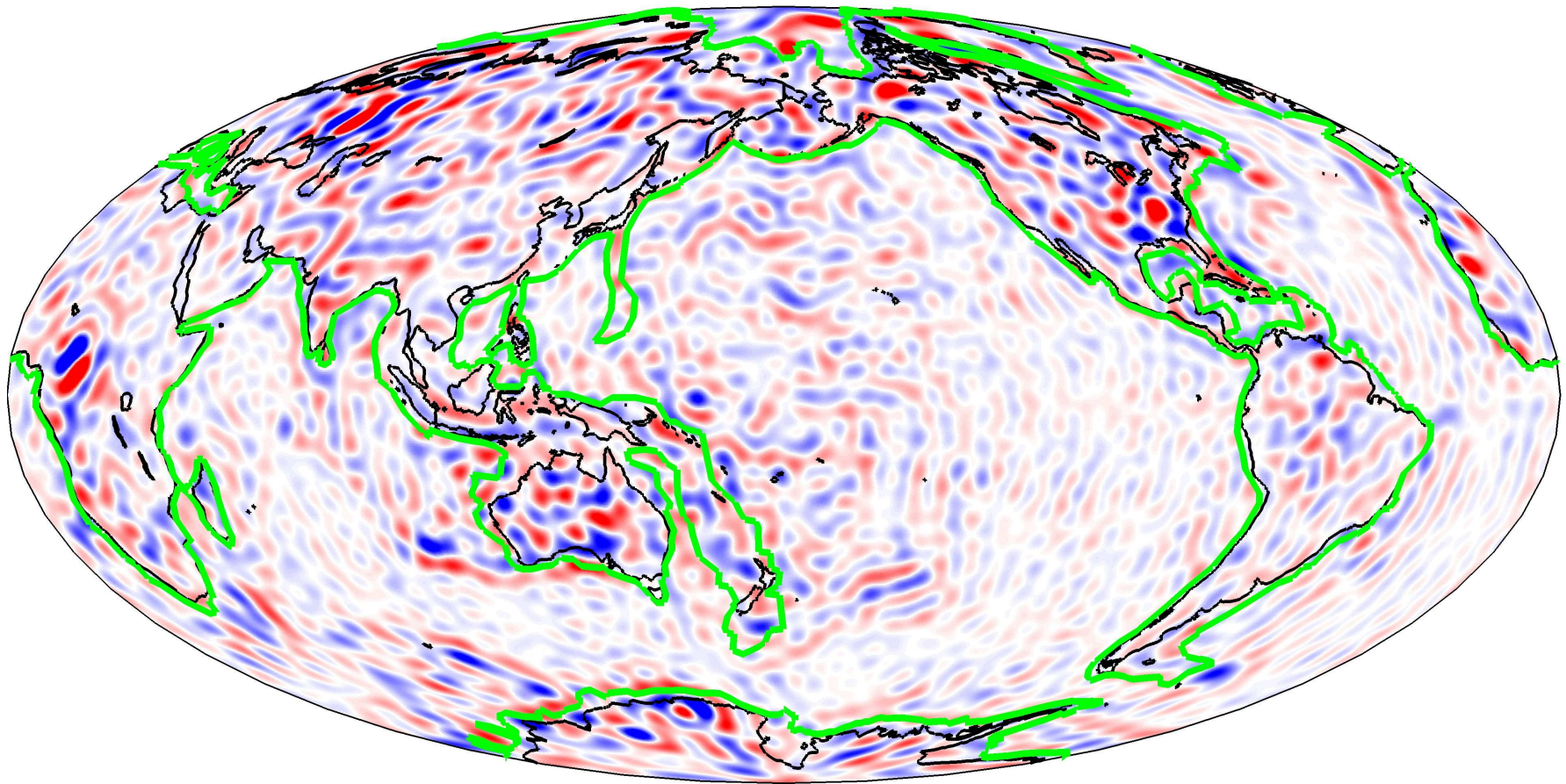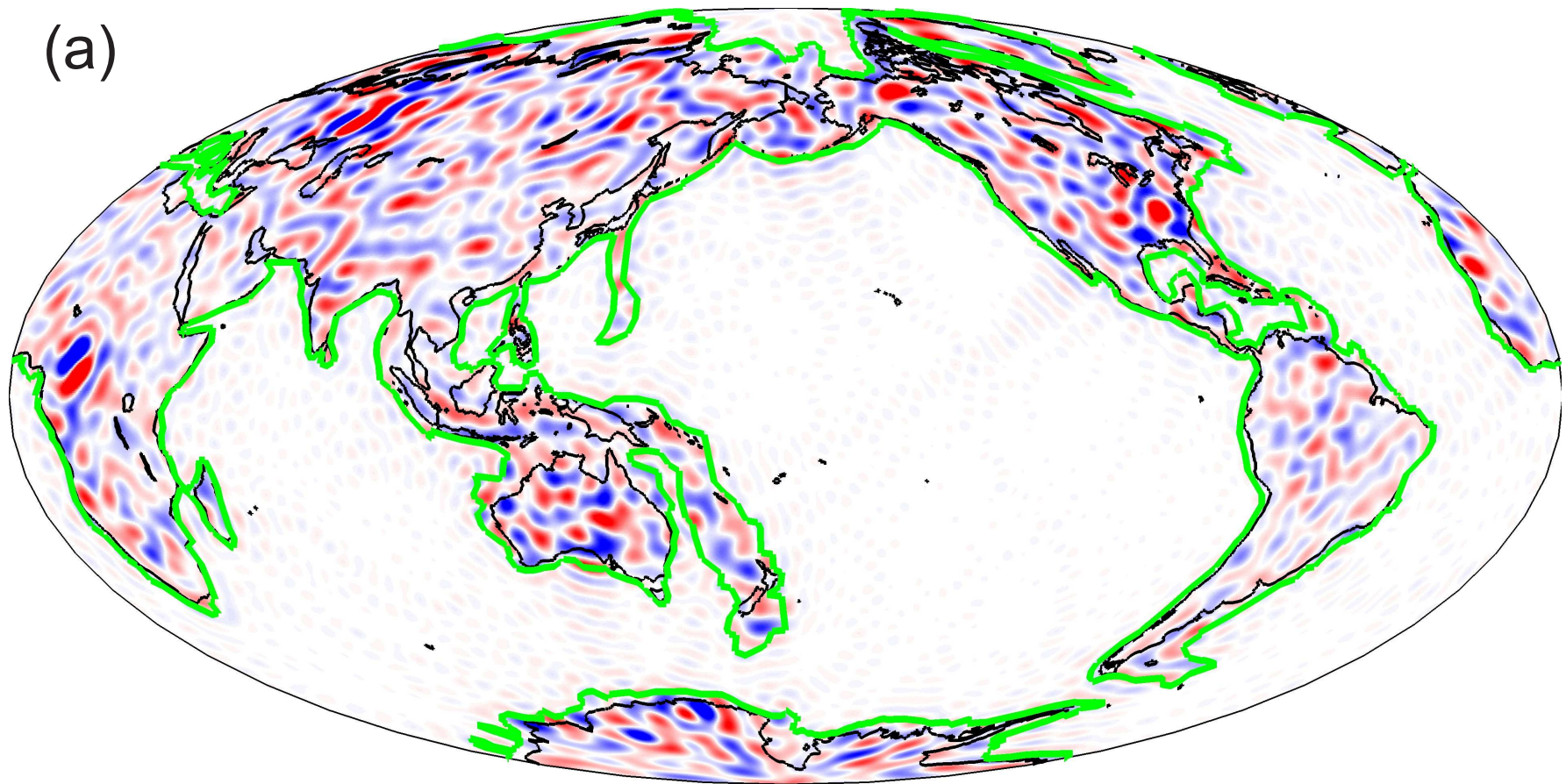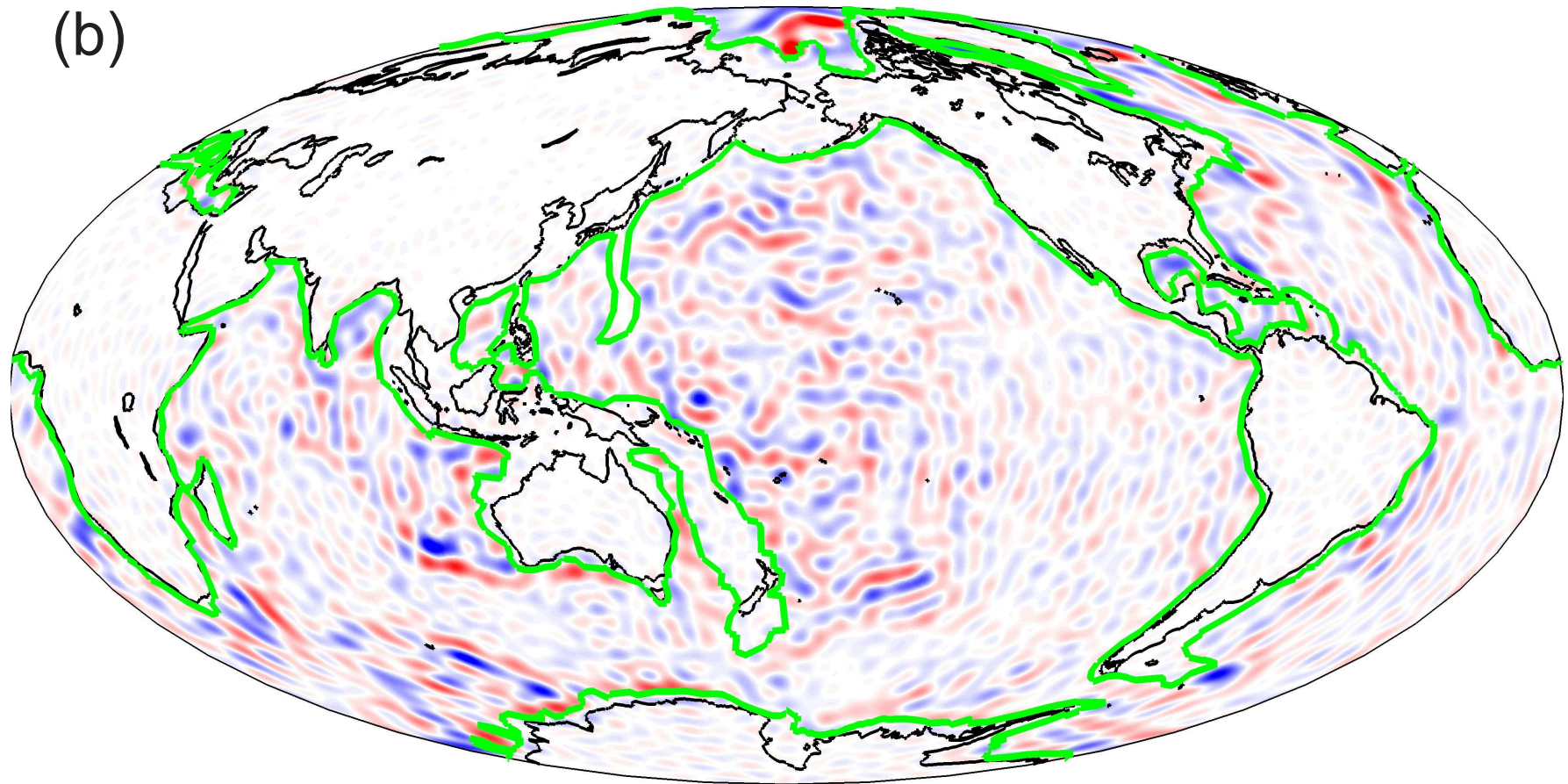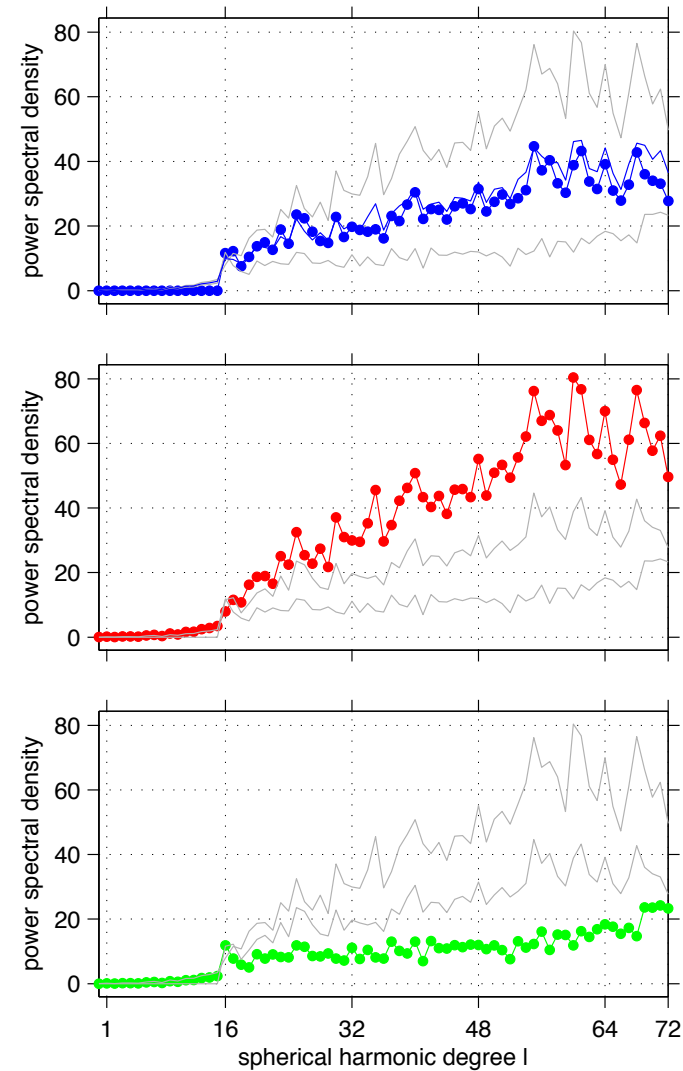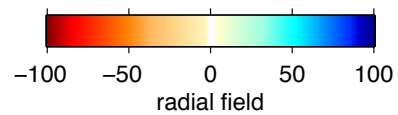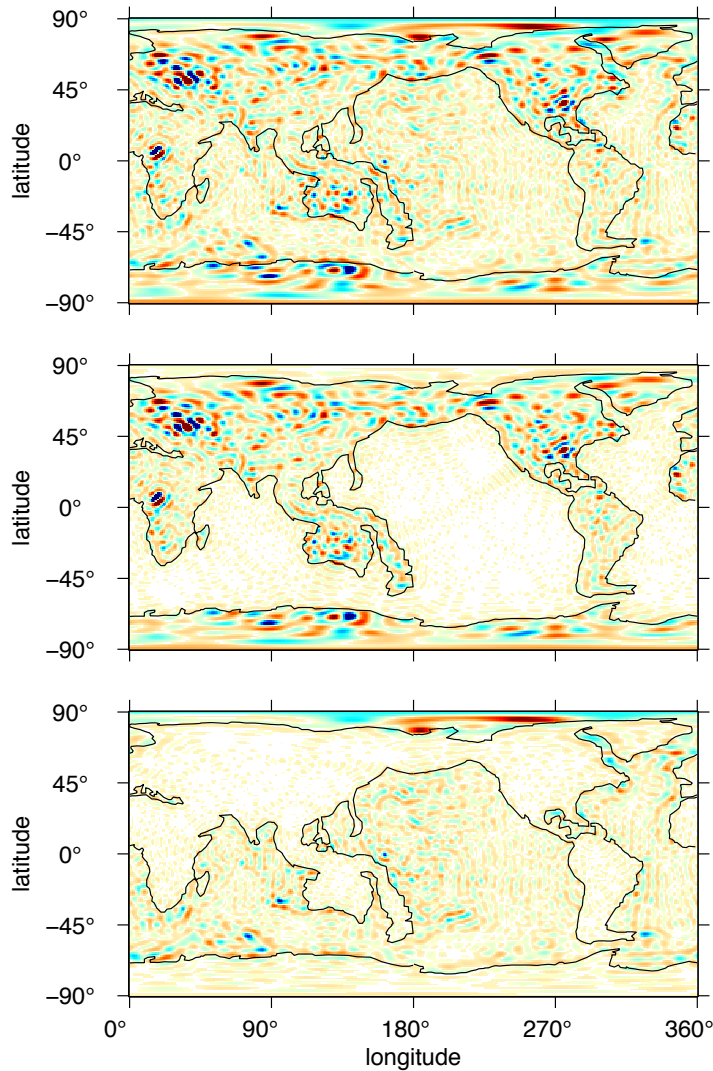
- Slepian functions are both spectrally and spatially **concentrated**

Summary: Linear & Quadratic Problems

- Slepian functions are both spectrally and spatially **concentrated**

- They form a **doubly orthogonal** basis on the sphere and any portion of it

Summary: Linear & Quadratic Problems

- Slepian functions are both spectrally and spatially **concentrated**

- They form a **doubly orthogonal** basis on the sphere and any portion of it

- They are the ideal basis to separate **signal** from noise, for **approximation** and **linear inverse problems**

Summary: Linear & Quadratic Problems

- Slepian functions are both spectrally and spatially **concentrated**

- They form a **doubly orthogonal** basis on the sphere and any portion of it

- They are the ideal basis to separate **signal** from noise, for **approximation** and **linear inverse problems**

- They are ideal data windows for **quadratic spectral analysis**

Summary: Linear & Quadratic Problems

- Slepian functions are both spectrally and spatially **concentrated**

- They form a **doubly orthogonal** basis on the sphere and any portion of it

- They are the ideal basis to separate **signal** from noise, for **approximation** and **linear inverse problems**

- They are ideal data windows for **quadratic spectral analysis**

- The **Slepian multitaper method** yields a smoothed and thus **biased** estimate of the spectrum, but it requires neither iteration nor large-scale matrix inversion. Its **variance is much lower** than that of any other method, and the only parameter that needs to be specified by the analyst is the **Shannon number**, or the space-bandwidth product diagnostic of the spatiospectral concentration.
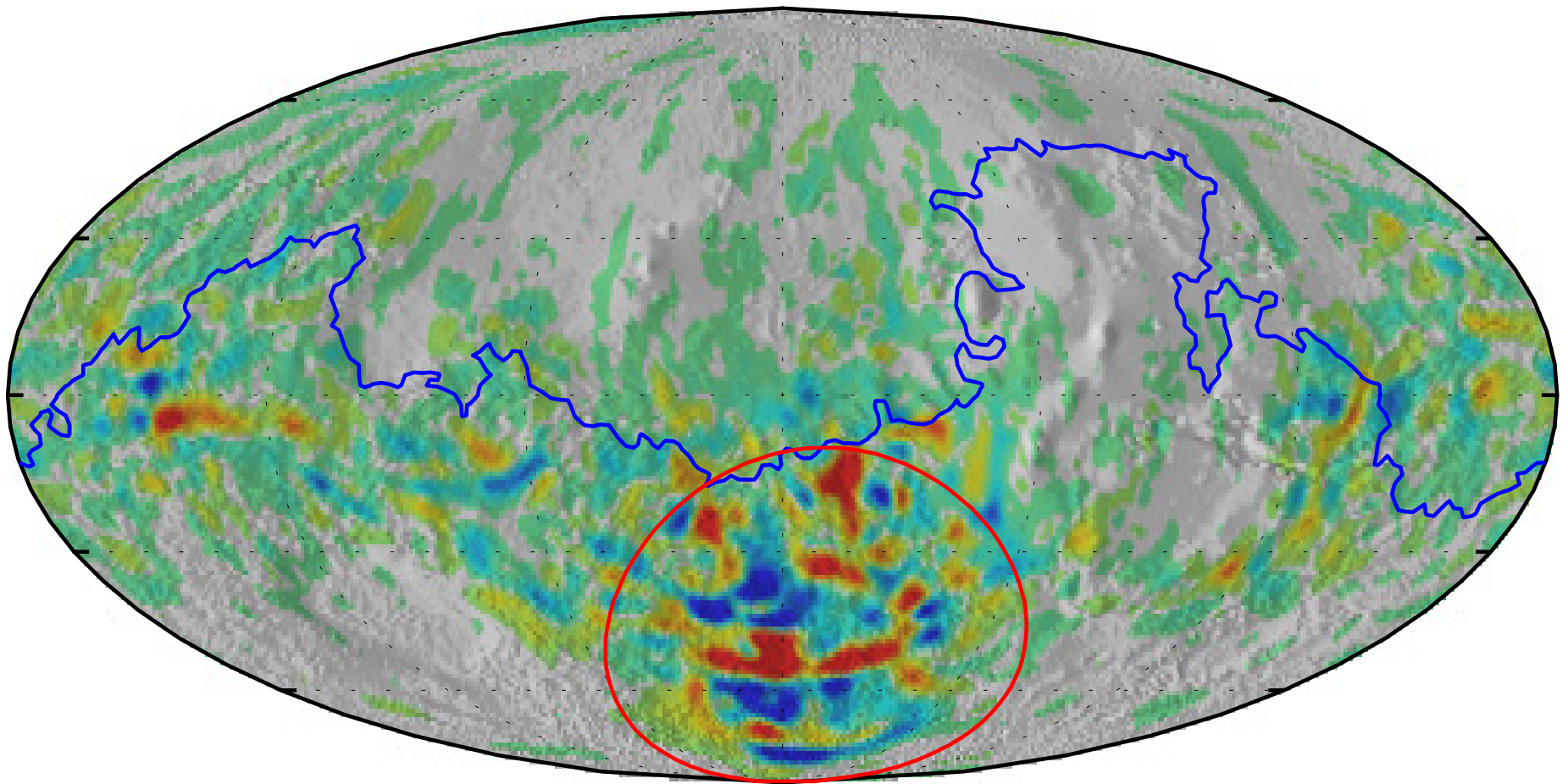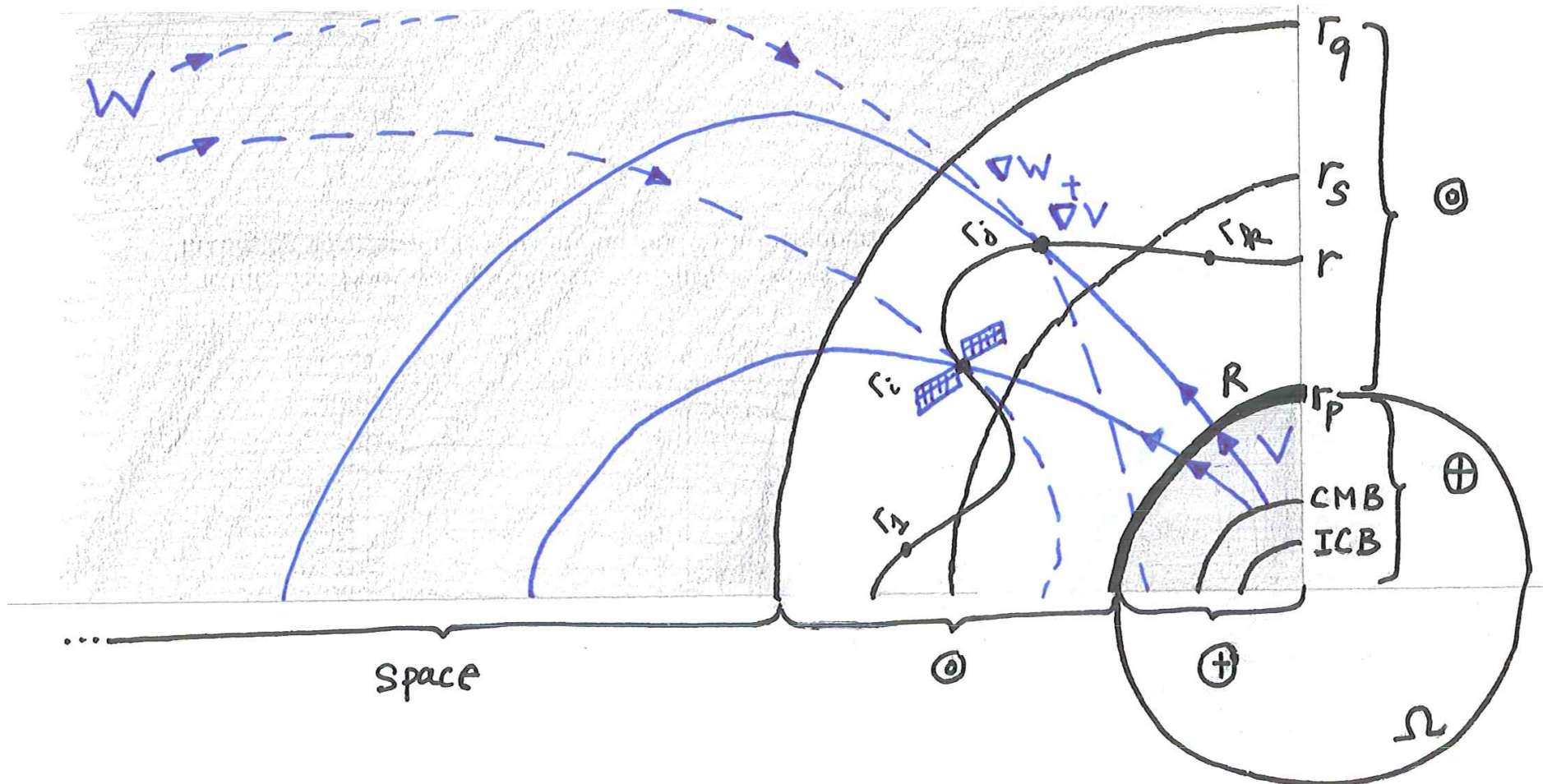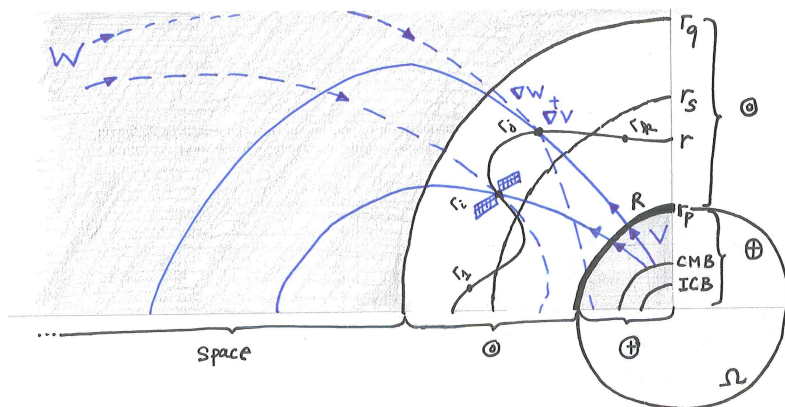
$$
d(r_s\hat{r}) =
\begin{cases}
\boldsymbol{\nabla} V(r_s\hat{r}) + \boldsymbol{\nabla} W(r_s\hat{r}) + \boldsymbol{n}(r_s\hat{r}) & \text{if } \hat{r} \in R \subset \Omega, \\
\text{unknown} & \text{if } \hat{r} \in \Omega \setminus R,
\end{cases}
\tag{19}
$$
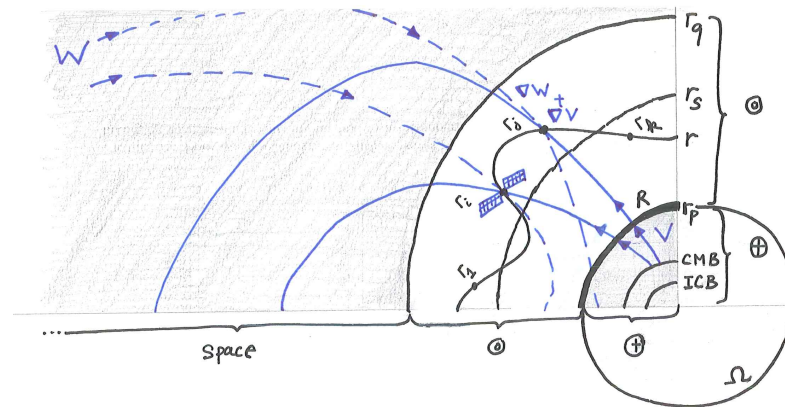
$$
\boldsymbol{d}(r_s\hat{\boldsymbol{r}}) =
\begin{cases}
\boldsymbol{\nabla} V(r_s\hat{\boldsymbol{r}}) + \boldsymbol{\nabla} W(r_s\hat{\boldsymbol{r}}) + \boldsymbol{n}(r_s\hat{\boldsymbol{r}}) & \text{if } \hat{\boldsymbol{r}} \in R \subset \Omega, \\
\text{unknown} & \text{if } \hat{\boldsymbol{r}} \in \Omega \setminus R,
\end{cases}
\tag{19}
$$

To obtain, from discrete satellite data collected within a confined region R at **varying altitude** above the planetary surface approximated by a sphere of radius r_p, the **bandlimited** set of coefficients $v_{lm}^{r_p} \in \mathrm{v}_L^{r_p}$, $0 \leq l \leq L$, that describe the **internal field** V on the planetary surface.

The $Y_{lm} \in \mathcal{Y}$ are the "regular" orthonormalized scalar *surface*-spherical harmonics, with $0 \leq l \leq \infty$ the angular **degree**, and $-l \leq m \leq l$ the angular **order**.

Scalar and vector spherical harmonics

The $Y_{lm} \in \mathcal{Y}$ are the "regular" orthonormalized scalar *surface*-spherical harmonics, with $0 \leq l \leq \infty$ the angular **degree**, and $-l \leq m \leq l$ the angular **order**.

The **inner** *solid* harmonics $r^l Y_{lm}$ are a basis for W, generated by **external** sources.

The $Y_{lm} \in \mathcal{Y}$ are the "regular" orthonormalized scalar *surface*-spherical harmonics, with $0 \leq l \leq \infty$ the angular **degree**, and $-l \leq m \leq l$ the angular **order**.

The **inner** *solid* harmonics $r^l Y_{lm}$ are a basis for W, generated by **external** sources.

The **outer** *solid* harmonics $r^{-l-1} Y_{lm}$ are a basis for V, from **internal** sources.

Scalar and vector spherical harmonics

The $Y_{lm} \in \mathcal{Y}$ are the "regular" orthonormalized scalar *surface*-spherical harmonics, with $0 \le l \le \infty$ the angular **degree**, and $-l \le m \le l$ the angular **order**.

The **inner** *solid* harmonics $r^l Y_{lm}$ are a basis for W, generated by **external** sources.

The **outer** *solid* harmonics $r^{-l-1} Y_{lm}$ are a basis for V, from **internal** sources.

We define *internal* and *external* **gradient vector spherical harmonics** (GVSH):

$$\boldsymbol{E}_{lm}(\hat{\boldsymbol{r}}) = \frac{1}{\sqrt{(l+1)(2l+1)}} \Big[\hat{\boldsymbol{r}} \, (l+1) \, Y_{lm}(\hat{\boldsymbol{r}}) - \boldsymbol{\nabla}_1 Y_{lm}(\hat{\boldsymbol{r}}) \Big], \quad (20)$$

The $Y_{lm} \in \mathcal{Y}$ are the "regular" orthonormalized scalar *surface*-spherical harmonics, with $0 \leq l \leq \infty$ the angular **degree**, and $-l \leq m \leq l$ the angular **order**.

The **inner** *solid* harmonics $r^l Y_{lm}$ are a basis for W, generated by **external** sources.

The **outer** *solid* harmonics $r^{-l-1} Y_{lm}$ are a basis for V, from **internal** sources.

We define *internal* and *external* **gradient vector spherical harmonics** (GVSH):

$$\boldsymbol{E}_{lm}(\hat{\boldsymbol{r}}) = \frac{1}{\sqrt{(l+1)(2l+1)}} \left[\hat{\boldsymbol{r}} \, (l+1) \, Y_{lm}(\hat{\boldsymbol{r}}) - \boldsymbol{\nabla}_1 Y_{lm}(\hat{\boldsymbol{r}}) \right], \quad (20)$$

$$\boldsymbol{F}_{lm}(\hat{\boldsymbol{r}}) = \frac{1}{\sqrt{l(2l+1)}} \left[\hat{\boldsymbol{r}} \, l \, Y_{lm}(\hat{\boldsymbol{r}}) + \boldsymbol{\nabla}_1 Y_{lm}(\hat{\boldsymbol{r}}) \right]. \quad (21)$$

The $Y_{lm} \in \mathcal{Y}$ are the "regular" orthonormalized scalar *surface*-spherical harmonics, with $0 \leq l \leq \infty$ the angular **degree**, and $-l \leq m \leq l$ the angular **order**.

The **inner** *solid* harmonics $r^l Y_{lm}$ are a basis for W, generated by **external** sources.

The **outer** *solid* harmonics $r^{-l-1} Y_{lm}$ are a basis for V, from **internal** sources.

We define *internal* and *external* **gradient vector spherical harmonics** (GVSH):

$$\boldsymbol{E}_{lm}(\hat{\boldsymbol{r}}) = \frac{1}{\sqrt{(l+1)(2l+1)}} \left[\hat{\boldsymbol{r}} \, (l+1) \, Y_{lm}(\hat{\boldsymbol{r}}) - \boldsymbol{\nabla}_1 Y_{lm}(\hat{\boldsymbol{r}}) \right], \quad (20)$$

$$\boldsymbol{F}_{lm}(\hat{\boldsymbol{r}}) = \frac{1}{\sqrt{l(2l+1)}} \left[\hat{\boldsymbol{r}} \, l \, Y_{lm}(\hat{\boldsymbol{r}}) + \boldsymbol{\nabla}_1 Y_{lm}(\hat{\boldsymbol{r}}) \right]. \quad (21)$$

Vector potentials $\boldsymbol{\nabla} V(r\hat{\boldsymbol{r}})$ are expanded into $\boldsymbol{E}_{lm}$ and the $\boldsymbol{\nabla} W(r\hat{\boldsymbol{r}})$ into $\boldsymbol{F}_{lm}$.

The $Y_{lm} \in \mathcal{Y}$ are the "regular" orthonormalized scalar *surface*-spherical harmonics, with $0 \leq l \leq \infty$ the angular **degree**, and $-l \leq m \leq l$ the angular **order**.

The **inner** *solid* harmonics $r^l Y_{lm}$ are a basis for W, generated by **external** sources.

The **outer** *solid* harmonics $r^{-l-1} Y_{lm}$ are a basis for V, from **internal** sources.

We define *internal* and *external* **gradient vector spherical harmonics** (GVSH):

$$\boldsymbol{E}_{lm}(\hat{\boldsymbol{r}}) = \frac{1}{\sqrt{(l+1)(2l+1)}} \left[\hat{\boldsymbol{r}} (l+1) Y_{lm}(\hat{\boldsymbol{r}}) - \boldsymbol{\nabla}_1 Y_{lm}(\hat{\boldsymbol{r}}) \right], \quad (20)$$

$$\boldsymbol{F}_{lm}(\hat{\boldsymbol{r}}) = \frac{1}{\sqrt{l(2l+1)}} \left[\hat{\boldsymbol{r}} l\, Y_{lm}(\hat{\boldsymbol{r}}) + \boldsymbol{\nabla}_1 Y_{lm}(\hat{\boldsymbol{r}}) \right]. \quad (21)$$

Vector potentials $\boldsymbol{\nabla} V(r\hat{\boldsymbol{r}})$ are expanded into $\boldsymbol{E}_{lm}$ and the $\boldsymbol{\nabla} W(r\hat{\boldsymbol{r}})$ into $\boldsymbol{F}_{lm}$.

We collect the basis functions into bandlimited sets $\mathcal{E}_L$ and $\mathcal{F}_{L_o}$.

The solution to the least-squares problem

$$\left(\begin{array}{cc} \mathbf{A} \displaystyle\int_{\mathcal{R}} \boldsymbol{\mathcal{E}}_L \cdot \boldsymbol{\mathcal{E}}_L^{\mathcal{T}} \, d\Omega \, \mathbf{A}^{\mathrm{T}} & \mathbf{A} \displaystyle\int_{\mathcal{R}} \boldsymbol{\mathcal{E}}_L \cdot \boldsymbol{\mathcal{F}}_{L_o}^{\mathcal{T}} \, d\Omega \, \check{\mathbf{A}}^{\mathrm{T}} \\[2ex] \check{\mathbf{A}} \displaystyle\int_{\mathcal{R}} \boldsymbol{\mathcal{F}}_{L_o} \cdot \boldsymbol{\mathcal{E}}_L^{\mathcal{T}} \, d\Omega \, \mathbf{A}^{\mathrm{T}} & \check{\mathbf{A}} \displaystyle\int_{\mathcal{R}} \boldsymbol{\mathcal{F}}_{L_o} \cdot \boldsymbol{\mathcal{F}}_{L_o}^{\mathcal{T}} \, d\Omega \, \check{\mathbf{A}}^{\mathrm{T}} \end{array} \right) \left(\begin{array}{c} \tilde{\mathrm{v}}_L^{r_p} \\[3ex] \tilde{\mathrm{w}}_{L_o}^{r_q} \end{array} \right) \begin{array}{l} \leftarrow \text{innies} \\[3ex] \leftarrow \text{outies} \end{array}$$

underbrace of the matrix:

This is $\mathring{\mathbf{K}}$.

We will work in the orthogonal eigenvector decomposition of this symmetric positive definite matrix:

$$\mathring{\mathbf{K}}\mathring{\mathbf{G}} = \mathring{\mathbf{G}}\mathring{\boldsymbol{\Lambda}}.$$

$$= \left(\begin{array}{c} \mathbf{A} \displaystyle\int_{\mathcal{R}} \boldsymbol{\mathcal{E}}_L \cdot \boldsymbol{d} \, d\Omega \\[4ex] \check{\mathbf{A}} \displaystyle\int_{\mathcal{R}} \boldsymbol{\mathcal{F}}_{L_o} \cdot \boldsymbol{d} \, d\Omega \end{array} \right).$$
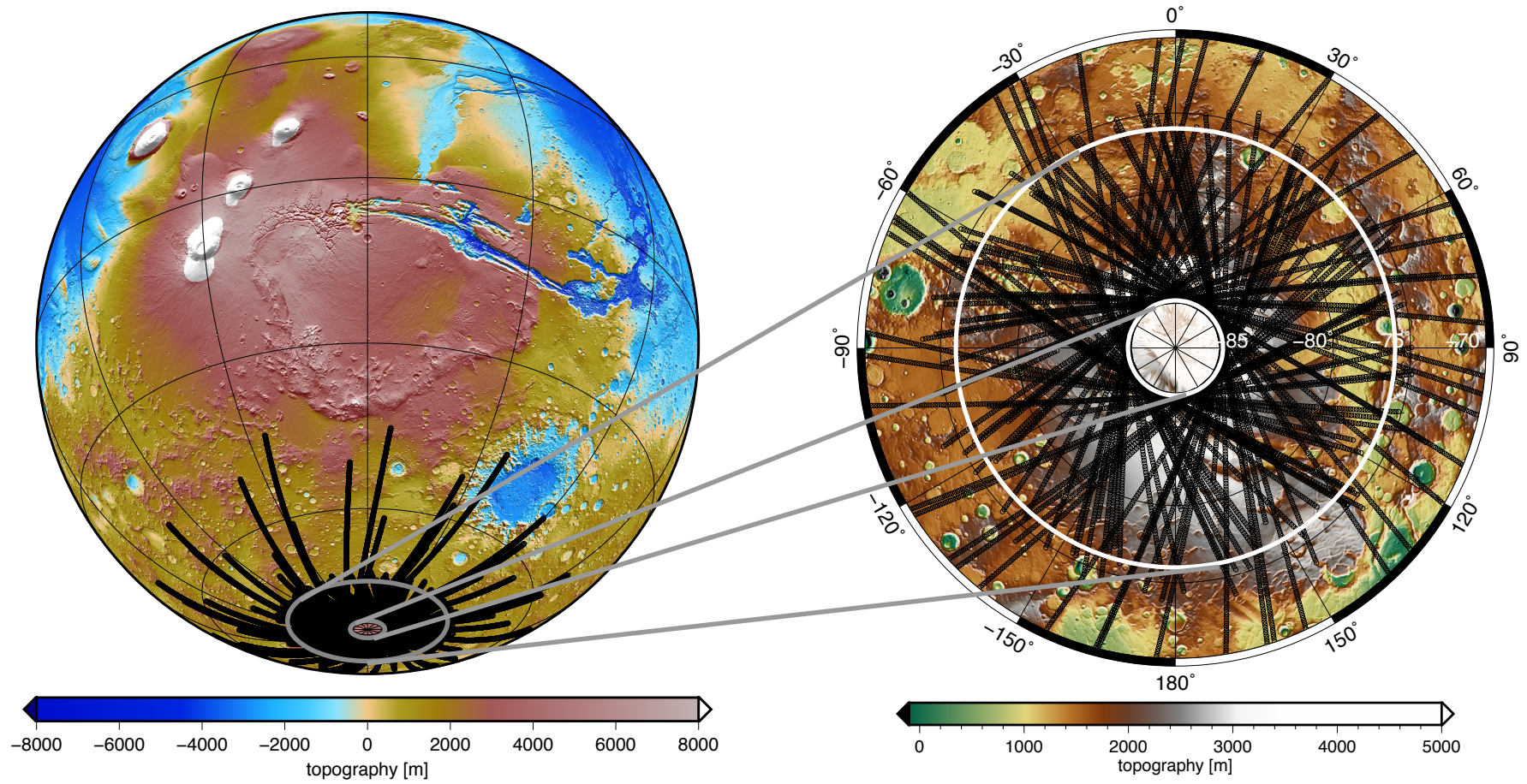
We obtained the full-field altitude-cognizant gradient-vector Slepian functions from solving a misfit-minimization problem by diagonalizing the matrix $\overset{\circ}{\mathbf{K}}$. The coefficients $\overset{\circ}{\mathbf{G}}$ can also be obtained by solving an energy maximization problem, as for the classical vector Slepian functions of *Plattner & Simons (2014)*.

Indeed we have solved the variational problem

$$\overset{\circ}{\lambda} = \frac{\overset{\circ}{g}^{\mathrm{T}} \overset{\circ}{\mathbf{K}} \overset{\circ}{g}}{\overset{\circ}{g}^{\mathrm{T}} \overset{\circ}{g}} = \frac{\left(\overset{\circ}{g}_i^{\mathrm{T}} \quad \overset{\circ}{g}_o^{\mathrm{T}} \right) \overset{\circ}{\mathbf{K}} \left(\overset{\circ}{g}_i^{\mathrm{T}} \quad \overset{\circ}{g}_o^{\mathrm{T}} \right)^{\mathrm{T}}}{\overset{\circ}{g}_i^{\mathrm{T}} \overset{\circ}{g}_i + \overset{\circ}{g}_o^{\mathrm{T}} \overset{\circ}{g}_o} \tag{22}$$

$$= \frac{\displaystyle\int_{\mathcal{R}} \overset{\circ}{\boldsymbol{G}}_{\uparrow}^2 \, d\Omega}{\displaystyle\int_{\Omega} \overset{\circ}{G}_i^2 \, d\Omega + \int_{\Omega} \overset{\circ}{G}_o^2 \, d\Omega}. \tag{23}$$
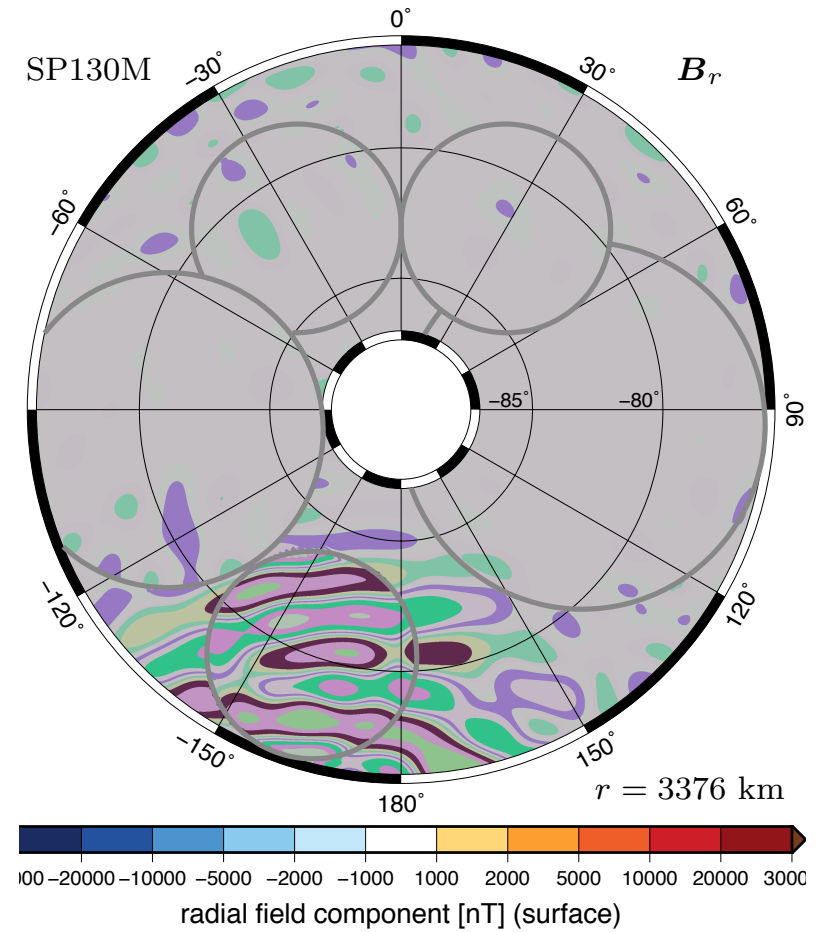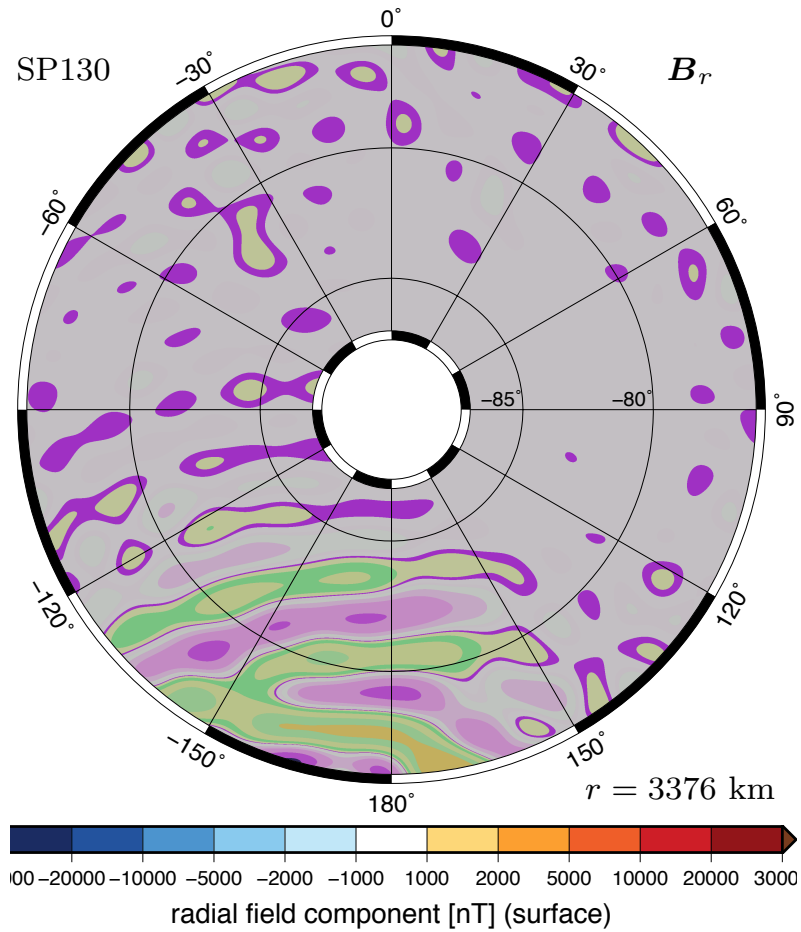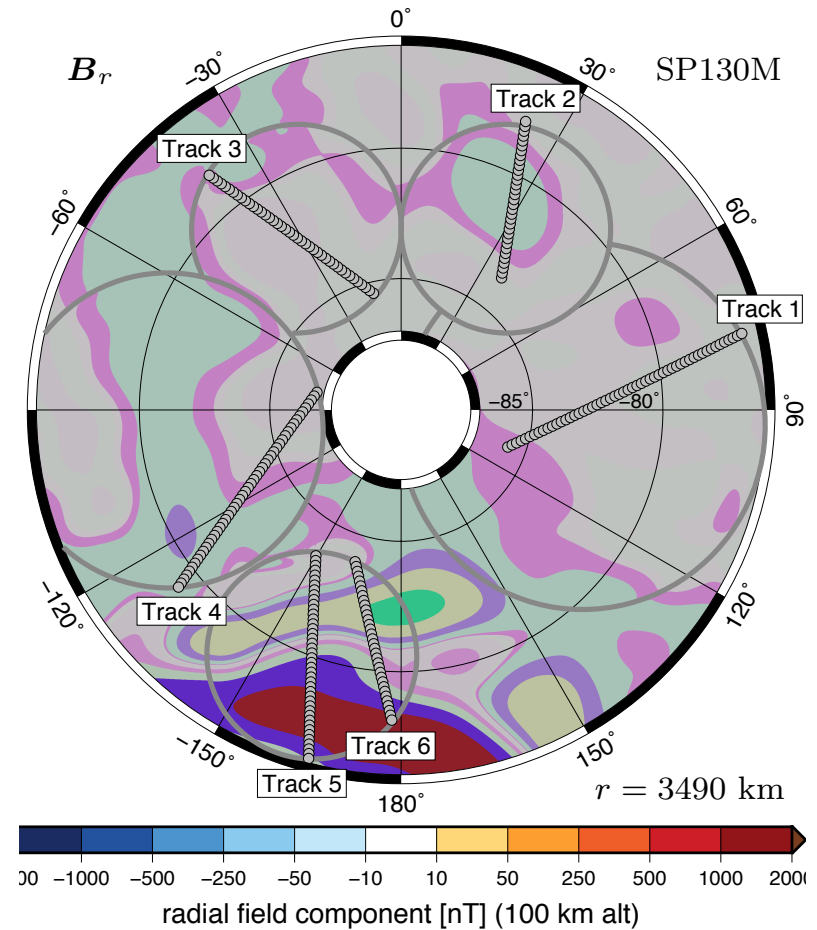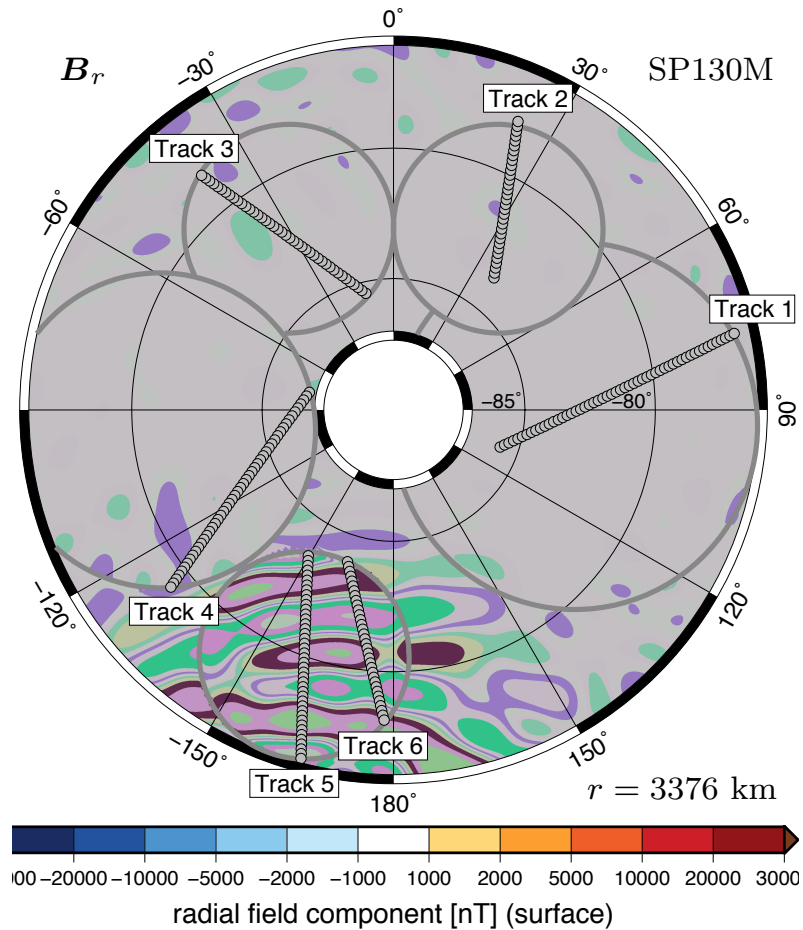
topography [m]

topography [m]

Finally! Conclusions

We solve inverse problems represented by a **linear and compact operator** between Hilbert spaces with a known **singular-value decomposition** (SVD). In practice, such an SVD is often only given for the case of a global expansion of the data (e.g., on the whole sphere) but not for regional data distributions.

We solve inverse problems represented by a **linear and compact operator** between Hilbert spaces with a known **singular-value decomposition** (SVD). In practice, such an SVD is often only given for the case of a global expansion of the data (e.g., on the whole sphere) but not for regional data distributions.

Slepian functions (associated to an arbitrarily prescribed region and the given compact operator) can be determined and applied to construct a regularization for the **ill-posed regional inverse problem**. We construct the Slepian basis by solving an algebraic eigenvalue problem.

Finally! Conclusions

We solve inverse problems represented by a **linear and compact operator** between Hilbert spaces with a known **singular-value decomposition** (SVD). In practice, such an SVD is often only given for the case of a global expansion of the data (e.g., on the whole sphere) but not for regional data distributions.

Slepian functions (associated to an arbitrarily prescribed region and the given compact operator) can be determined and applied to construct a regularization for the **ill-posed regional inverse problem**. We construct the Slepian basis by solving an algebraic eigenvalue problem.

The obtained Slepian functions can be used to derive an SVD for the combination of the **regionalizing projection** and the compact operator.

Finally! Conclusions

We solve inverse problems represented by a **linear and compact operator** between Hilbert spaces with a known **singular-value decomposition** (SVD). In practice, such an SVD is often only given for the case of a global expansion of the data (e.g., on the whole sphere) but not for regional data distributions.

Slepian functions (associated to an arbitrarily prescribed region and the given compact operator) can be determined and applied to construct a regularization for the **ill-posed regional inverse problem**. We construct the Slepian basis by solving an algebraic eigenvalue problem.

The obtained Slepian functions can be used to derive an SVD for the combination of the **regionalizing projection** and the compact operator.

Standard **regularization techniques** relying on a known SVD become applicable also to those inverse problems where the data are regionally given only.

Eigenvalue weighted SPATIAL sum

Eigenvalue weighted SPECTRAL sum

$\alpha = 1 \mid \lambda = 0.99932$ $\alpha = 2 \mid \lambda = 0.99923$ $\alpha = 3 \mid \lambda = 0.99833$